InSAR Water Vapor Data Assimilation into Mesoscale Model MM5: Technique and Pilot Study

Emanuela Pichelli, Rossella Ferretti, Domenico Cimini, Giulia Panegrossi, Daniele Perissin, Nazzareno Pierdicca, *Senior Member, IEEE*, Fabio Rocca, and Bjorn Rommen

***Abstract*—In this study, a technique developed to retrieve integrated water vapor from interferometric synthetic aperture radar (InSAR) data is described, and a three-dimensional variational assimilation experiment of the retrieved precipitable water vapor into the mesoscale weather prediction model MM5 is carried out. The InSAR measurements were available in the framework of the European Space Agency (ESA) project for the "Mitigation of electromagnetic transmission errors induced by atmospheric water vapor effects" (METAWAVE), whose goal was to analyze and possibly predict the phase delay induced by atmospheric water vapor on the spaceborne radar signal. The impact of the assimilation on the model forecast is investigated in terms of temperature, water vapor, wind, and precipitation forecast. Changes in the modeled dynamics and an impact on the precipitation forecast are found. A positive effect on the forecast of the precipitation is found for structures at the model grid scale or larger (1 km), whereas a negative effect is found on convective cells at the subgrid scale that develops within 1 h time intervals. The computation of statistical indices shows that the InSAR assimilation improves the forecast of weak to moderate precipitation (<15 mm/3 h).**

***Index Terms*—Atmospheric path delay, data assimilation, numerical weather prediction (NWP), synthetic aperture radar (SAR), water vapor.**

I. Introduction

ONE OF THE major error sources in the short-term forecast of precipitation is the lack of precise and continuous measurements of water vapor data [1], [2]. The water vapor is an extremely important element of the atmosphere because its distribution is related to clouds, precipitation formation, and it represents a large proportion of the energy budget in the atmosphere. Its representation inside numerical weather prediction (NWP) models is critical to improve the weather forecast. It is also very challenging because water vapor is involved in processes over a wide range of spatial and temporal scales. An improvement in atmospheric water vapor monitoring that can be assimilated in NWP models would improve the forecast accuracy of precipitation and severe weather [1], [3]. In this framework, the spaceborne interferometric synthetic aperture radar (InSAR), a useful tool for high-resolution water vapor retrieval [4], represents an interesting source of data to be assimilated into mesoscale models. Panegrossi *et al.* [5] have demonstrated the InSAR capability of providing soil moisture maps to constrain the surface boundary conditions in NWP models. InSAR is based on the measurement of the phase differences, associated with the distance between the satellite and each land surface element, as observed from different satellite positions or at different times [6]. The neutral atmosphere introduces an unknown delay in the SAR signal propagation, particularly, due to the high water vapor spatial and temporal variability. Due to the differential nature of the InSAR technique, the tropospheric contribution to the SAR interferogram, i.e., the so-called atmospheric phase screen (APS), is actually related to the difference of delays due to the atmosphere when SAR signals propagate through it, rather than their absolute value [7]. This effect can be exploited, offering a potential source of integrated water vapor (IWV) data (i.e., precipitable water) with a high spatial resolution, provided that the ground motion and topography effects are removed to isolate the water vapor contribution [3].

This paper presents a numerical experiment carried out by a variational data assimilation system (3DVAR) to assimilate InSAR observations into the Pennsylvania State University mesoscale model MM5 and to test their impact on the forecast. The InSAR data used in the assimilation were collected during the 2008 campaign of the ESA project METAWAVE (Mitigation of electromagnetic transmission errors induced by atmospheric water vapor effects) [8]. In this project, the effect of water vapor path delay in InSAR applications was deeply investigated, trying to identify and compare possible independent sources of information valuable to mitigate those artifacts [3], [8]–[13]. Several methods and tools have been exploited in order to retrieve the water vapor field and related characteristics at resolution suitable for mitigating its effect on InSAR.

Manuscript received February 13, 2014; revised July 04, 2014; accepted September 01, 2014. This work was supported in part by the European Space Agency under contract N. ESTEC-21207/07/NL/HE.

E. Pichelli and R. Ferretti are with the Department of Physics and Chemistry, CETEMPS, University of L'Aquila, 67100 L'Aquila, Italy (e-mail: emanuela.pichelli@aquila.infn.it; rossella.ferretti@aquila.infn.it).

D. Cimini is with the Institute of Methodologies for Environment Analysis, CNR, 85050 Potenza, Italy, and also with the Department of Physics and Chemistry, CETEMPS, University of L'Aquila, 67100 L'Aquila, Italy (e-mail: cimini@imaa.cnr.it).

G. Panegrossi is with the Institute of Atmospheric Sciences and Climate, CNR, 00133 Rome, Italy (e-mail: giulia.panegrossi@artov.isac.cnr.it).

D. Perissin is with the School of Civil Engineering, Purdue University, West Lafayette, IN 47907 USA (e-mail: perissin@purdue.edu).

N. Pierdicca is with the Department of Information Engineering, Electronics and Telecommunications, Sapienza University of Rome, 00184 Rome, Italy (e-mail: pierdicca@die.uniroma1.it).

F. Rocca is with the DEI, Politecnico di Milano, 20133 Milan, Italy (e-mail: rocca@elet.polimi.it).

B. Rommen is with the European Space Research and Technology Centre, European Space Agency (ESTEC/ESA), 2200AG Noordwijk, The Netherlands (e-mail: Bjorn.Rommen@esa.int).

Color versions of one or more of the figures in this paper are available online at http://ieeexplore.ieee.org.

Digital Object Identifier 10.1109/JSTARS.2014.2357685

In this work, we try to turn the InSAR tropospheric noise into an opportunity for NWP models. A major difficulty is the differential nature of the APS data (in time and space). APS provides high-resolution mapping of the atmospheric path delay changes with time where the earth surface remains steady, but they do not furnish absolute values. This is a relevant drawback if APSs are sampled at long time intervals, as in the case of the radar aboard the Envisat satellite, thus preventing, for instance, four-dimensional (4-D) variational assimilation. However, the revisit time is going to increase to the order of few days (as for COSMO-SkyMed and Sentinel 1) thanks to the emerging constellations of radar sensors and could even become to the order of hours considering the possibility to deploy a SAR aboard a geostationary orbit [14].

The goal of this study is to verify if the assimilation of IWV data retrieved from InSAR have an impact on numerical weather forecasts, and to be able to assess if the impact is positive and if the precipitation forecast improves.

Previous studies demonstrated that the assimilation of IWV leads to better initial conditions (ICs) and that the retrieval of vertical structure of water vapor from observed data can improve the precipitation forecast, especially if it is associated with the assimilation of wind observations [2].

The lack of the absolute value of IWV data using APS can be partially solved by merging the high-resolution differential information with a smoothed background provided by a statistical analysis of water vapor map temporal series. In this way, the high-resolution APS information, estimated from the Advanced SAR (ASAR) aboard of the Envisat satellite (by using the Permanent Scatterer (PS) multipass technique [15]), can be used to NWP models' ICs. The methodology used to face this problem and the obtained results are described in Section II.

Section III presents an overview of the case study (October 3, 2008) that corresponds to one of the two overpasses of Envisat collected during the 15-day METAWAVE campaign. Different measurements were available for comparison and validation of the results, including vertical profiles of thermodynamical variables and radar data of reflectivity and precipitation. Unstable conditions of that day allowed to evaluate the impact of the assimilation also on the precipitation, one of the most difficult field to be predicted.

The NWP model configuration and a brief summary of the assimilation method are described in Section IV. Results of the assimilation experiment and their discussion are presented in Section V. The model results after assimilation of IWV retrieved from APSs are compared to a control simulation (without any kind of assimilation) to evaluate its impact on the simulation. Radio soundings, meteorological radar, and rain gauges observations are used as reference. The conclusion of this study is summarized in Section VII.

II. IWV Maps From InSAR

The first problem to be solved to assimilate InSAR APS data is to obtain the absolute IWV value. The atmospheric delay measured by the SAR has been scaled according to its observation angle (19.2°–26.7°) to find correspondence with the vertical profiles of MM5, and a zenith-equivalent atmospheric delay is considered hereafter.

The derivation of absolute IWV from InSAR is not straightforward, as an interferogram from SAR is proportional to the path delay difference in both time and space [16], and the InSAR APS at any given time is obtained by removing the uncorrelated noise and a phase ramp (i.e., a bilinear function of the image coordinates which can originate from satellite orbit errors). Beside the conversion from path delay to IWV, which can be assumed roughly based on a proportionality factor [13], the basic idea is to estimate the time average distribution of IWV in a given area and within a time frame by relying on an external source, such as IWV maps from other earth observation (EO) sensors.

The interferometric phase at a point $\mathbf{r} = [x, y]$ in the image represents the phase difference between two SAR overpasses (at time i and j, respectively) referred to a single point $\mathbf{r}_0$. It contains a surface displacement term (subscript *DISPL*) and a term due to atmospheric path delay distortions (subscript *ATMO*). The image acquisition's time difference is indicated by Δ_{ij}, Φ denotes the phase, and L is the path delay; for a SAR interferogram, we can write

$$\Delta_{ij}\Phi(\mathbf{r}) - \Delta_{ij}\Phi(\mathbf{r}_0) = \Delta_{ij}\Phi_{DISPL}(\mathbf{r}) + \frac{4\pi}{\lambda}\Delta_{ij}L_{ATMO}(\mathbf{r}) - \Delta_{ij}\Phi(\mathbf{r}_0) \tag{1}$$

where the one-way atmospheric path delay L and phase are simply related by the wave number $k = 2\pi/\lambda$ multiplied by 2 to consider the radar signal round-trip, where λ is the wavelength. In clear sky conditions, the path delay L has a hydrostatic dry term and a term which is approximately proportional to IWV through a factor Π (i.e., $L = \mathrm{IWV}/\Pi$). It can be demonstrated that this factor is roughly 0.15 (slightly depending on conditions), so that 1 mm of IWV corresponds to roughly 6 mm of path delay due to water vapor [13].

For a nondeforming earth surface or a surface whose deformation can be modeled, $\Delta_{ij}\Phi_{DISPL}$ can be removed. The atmospheric delay disturbance (or APS) can be produced in each point $\mathbf{r}$ by differencing a sequence of SAR images with respect to a master image taken at time $j = \mathrm{M}$, with an arbitrary unknown constant (const_i) corresponding to the phase difference of the reference point x_0, i.e., $\mathrm{const}_i = \lambda \cdot \Delta\Phi_{iM}(\mathbf{r}0)/4\pi$

$$\mathrm{APS}_i(\mathbf{r}) = L_i(\mathbf{r}) - L_M(\mathbf{r}) - \mathrm{const}_i. \tag{2}$$

In (2), we can assume that the hydrostatic component is constant within a typical SAR image (i.e., it is assumed that there are no significant changes in the surface pressure and temperature fields within the extension of the image which is less than 100 km). The hydrostatic component is thus included into const_i, and the remaining path delay is mainly related to IWV.

However, the decreasing path delay over mountain sites, due to the shorter distance traveled through the atmosphere, is also related to the vertical stratification of the atmosphere [13]. Basili *et al.* [13] show that the trend of wet path delay with respect to surface height ranges from 1 cm/km for a dry atmosphere to more than 5 cm/km for a very moist atmosphere. The dry path delay also contributes to this trend, but its changes are assumed to be much lower.

Thus, in order to derive an absolute value of the path delay at a given time i from the APS, one should know the atmospheric conditions at the time of the master image acquisition (i.e., L_M), though the ambiguity associated with const_i remains. L_M could be provided by other sources, e.g., the EO sensors sensitive to water vapor content, either in the infrared or microwave spectral band. The NWP outputs could provide L_M to estimate L_i, but these cannot be used when attempting to assimilate the absolute APS, as it would introduce statistically correlated observations into the assimilation process. Thus, the error variance associated with the water vapor content of the master acquisition provided by the external source (σ^2_{EXT}) can be significant. This would add up to the APS intrinsic error (σ^2_{APS}) resulting in the error variance of the estimated IWV at time i ($\sigma^2{}_{IWV}$)

$$\sigma^2_{\mathrm{IWV}_i} = \sigma^2_{\mathrm{EXT}} + \sigma^2_{\mathrm{APS}_i}. \tag{3}$$

If a suitable sequence of external data was available, another approach could be followed by averaging many APS images and relying on the external source to estimate the expected value of the atmosphere path delay (assuming that the SAR and the external sources are observing *on average* the same atmosphere). We would have

$$\text{Mean}\left[\mathrm{APS}_i(\mathbf{r})\right] = \text{Mean}\left[L_i^{\mathrm{EXT}}(\mathbf{r})\right] - L_M(\mathbf{r}) - \text{const}$$

from which we can estimate the master to be substituted into (2), and thus more reliably estimate the absolute atmospheric delay from APS as

$$L_i(\mathbf{r}) = \mathrm{APS}_i(\mathbf{r}) - \text{Mean}\left[\mathrm{APS}_i(\mathbf{r})\right] + \text{Mean}\left[L_i^{\mathrm{EXT}}(\mathbf{r})\right] + \mathrm{const}_i. \tag{4}$$

Note that for each time i, there is still an unknown constant which can be estimated from the external source at that specific time, as it is explained below. The advantage of (4) is in the lower influence of the external source errors, as the error variance of the mean estimates is reduced by a factor equal to the number of available observations used in the averaging process, which should be very large

$$\sigma^2_{\mathrm{IWV}_i} = \sigma^2_{\text{Mean EXT}} + \sigma^2_{\text{Mean APS}} + \sigma^2_{\mathrm{APS}_i}. \tag{5}$$

In our experiment, the external source to estimate the IWV comes from the MEdium Resolution Imaging Spectrometer (MERIS) aboard Envisat, which provides images simultaneously to the ASAR acquisitions. Note that clouds affect IWV estimation from MERIS; therefore, the MERIS operational cloud mask is used for discarding cloud-contaminated pixels. In spite of this, when performing the averaging of many APS maps required in (4), the mean background maps become available everywhere in the SAR frame (assuming clear-sky conditions for at least few cases in the stack). From the absolute path delay retrieved as in (4), the IWV is finally derived

$$\mathrm{IWV}_i^{\mathrm{APS}}(\mathbf{r}) = \Pi L_i(\mathbf{r}) = \Pi(\lambda/4\pi)\Phi_i(\mathbf{r}). \tag{6}$$

Note that (6) is still wrapped, hence the 2π phase ambiguity affecting the APS should be added. Since ASAR works at 5.3 GHz, in this specific case, the 2π phase ambiguity corresponds to a variation in the slant path delay that folds one wavelength $\lambda = 5.66$ cm; considering that the observing angle is $\theta_z = 19.2^\circ - 26.7^\circ$ and that the SAR signal travels the atmosphere twice, this slant path delay corresponds to a variation in IWV equal to $\mathrm{dIWV} = \lambda/2\sec(\theta_z) * \Pi \approx 0.40 \pm 0.01$ cm. Thus, the APS 2π phase ambiguity maps into a IWV ambiguity approximately equal to $\mathrm{dIWV}^{2\pi} \sim 0.40$ cm. However, APS may also be affected by a phase ramp, which consists of a phase residual associated with orbital errors showing a linear trend with the position on a horizontal plane x, y (i.e., East and North coordinates in the map). If information about the IWV field is coming from an external source (e.g., MERIS in our case), the constant term, the 2π phase ambiguity, and the phase ramp can be removed. A simple two-step process is used to remove these terms: 1) search for the two-dimensional (2-D) east/north planar trend in the difference between $\mathrm{IWV}_i^{\mathrm{EXT}}$ and $\mathrm{IWV}_i^{\mathrm{APS}}$ (assuming $\mathrm{const}_i = 0$) and 2) remove the obtained plane from $\mathrm{IWV}_i^{\mathrm{APS}}$, i.e.,

$$\begin{aligned}\mathrm{IWV}_i^{\mathrm{APS}} = \Pi\left\{\mathrm{APS}_i(\mathbf{r}) - \text{Mean}\left[\mathrm{APS}_i(\mathbf{r})\right]\right\} \\ + \text{Mean}\left[\mathrm{IWV}_i^{\mathrm{EXT}}(\mathbf{r})\right] + F^i(x,y)\end{aligned} \tag{7}$$

$$\begin{aligned} F^i(x,y) &= a_o^i + a_x^i \cdot x + a_y^i \cdot y \\ \left[a_o^i, a_x^i, a_y^i\right] &= \mathrm{FIT}_{2D}\left\{\mathrm{IWV}_i^{\mathrm{EXT}}(\mathbf{r}) - \Pi\cdot\left\{\mathrm{APS}_i(\mathbf{r})\right.\right. \\ &\quad \left.\left. - \text{Mean}\left[\mathrm{APS}_i(\mathbf{r})\right]\right\} - \text{Mean}\left[\mathrm{IWV}_i^{\mathrm{EXT}}(\mathbf{r})\right]\right\}\end{aligned} \tag{8}$$

where $\mathrm{FIT}_{\mathrm{2D}}$ represents a two-dimentional least square fitting operator.

However, an extensive cloudiness can reduce the number of pixels with a meaningful IWV, and thus it could preclude the trend estimation. In addition, MERIS IWV may appear under/overestimated in the presence of undetected cloudy pixels (e.g., at cloud edges) or pixels under cloud shadows, respectively [17]. Some measures have been adopted to reduce the risk of affecting the trend estimation. The most stringent cloud mask provided by MERIS has been considered for discarding all the pixels that are detected as cloudy or undetermined at any rate. This eliminates the pixels where the IWV is not provided, and it also reduces the chances for cloud edges and cloud shadow. Then, the trend estimation is applied only if MERIS data are plenty ($> 50\%$ of the domain area) and approximately evenly distributed.

In conclusion, in this approach, the APS brings information on the high spatial frequency component of the path delay, whereas the low frequency component still needs to be provided by other sources of information (like independent model analysis or EO products, such as MERIS in our case).

III. Overview of the Case Study

Within the framework of the METAWAVE project, a comparison between ENVISAT interferograms and NWP model runs was performed for a period of several years for the area of Rome (Central Italy) and Como (Northern Italy).

During Autumn 2008, the experimental campaign took place and lasted for about 15 days. Microwave radiometers, radio soundings, and GPS receivers were deployed both in Rome and Como areas, and data from available satellites and GPS receiver operational networks were regularly collected to perform a comparison exercise [11]. During that period, Envisat overpassed the experiment area in Rome twice, collecting images, respectively, from an ascending and descending orbit. One of the days of the experimental campaign is used for this study: October 3, 2008, for its unstable meteorological conditions, represents a significant test case for studying the assimilation impact on precipitation.

During October 3, 2008, a cold front associated with a North Atlantic cyclone crossed over Italy, followed by an anticyclone entering from the west side of the Mediterranean basin (not shown). The radio soundings in Pratica di Mare (South west of Rome, 41.65°N, 12.43°E) showed a weakly unstable atmosphere at 00 UTC (Fig. 1, top panel) with south-westerly winds at the surface and westerly winds at upper levels. The instability increased in the following hours and a south-southwesterly wind component was detected, as shown in the radio sounding of 12 UTC of the same day (Fig. 1, bottom panel). The incoming cold air mass contributed to increase the humidity of the middle atmosphere during the day (in Fig. 1, the dew point temperature at 12 UTC is closer to the temperature curve than in the previous profile in the layer between 850 and 600 hPa) increasing its instability [the convective available potential energy (CAPE) grows from almost 16.7 J/kg up to 67.7 J/kg]. The decrease of the lifted index (LIFT) and the increase of the K-index (KINX) indicate the increasing probability of widely scattered thunderstorms occurrence over the region.

The Doppler radar located on the *Midia* mountain (42.05°N, 13.17°E) recorded echoes from 12 UTC off the coast southwest of Rome (not shown); in the following 2 h, scattered cells with reflectivity between 15 and 35 dBz (equivalent to rainfall rate up to 6 mm/h) were detected over most of the southern part of Lazio [between the cities of Latina (LT) and Frosinone (FR), top left panel of Fig. 2]; after 16 UTC precipitation was observed also in the innermost territory east of Rome (Fig. 2, top right panel). Some localized cells exceeding 35 dBz were found at 17 UTC (not shown). Finally, moderate to locally heavy rain cells were detected between 20 and 21 UTC (Fig. 2, bottom panels), with localized maxima of 40–45 dBz (12–24 mm/h of rainfall); after this time, rain gradually decreased, ending by midnight.

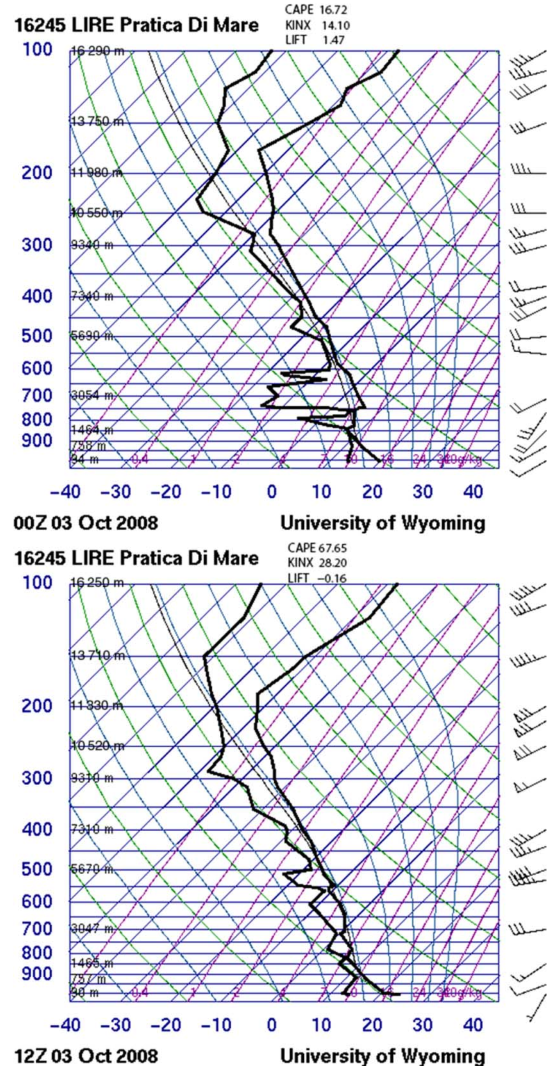

Fig. 1. Radio soundings from Pratica di Mare, at the center of the coast of Lazio, Central Italy, at 00 UTC of October 3, 2008 (top) and at 12 UTC (bottom). The two black lines represent, respectively, the dew point temperature (°C, left) and the temperature (°C, right). Wind barbs are plotted on the right (Data available on weather.uwyo.edu).

IV. Model Configuration and Data Assimilation Technique

A. MM5 Configuration

The fifth generation of National Center for Atmospheric Research (NCAR) and Pennsylvania State University (PSU) mesoscale model (MM5) is used in this study. This is a nonhydrostatic model at primitive equations with a terrain-following vertical coordinate and multiple nesting capabilities [18]. Four two-way nested domains are used to simulate the weather event on October 3, 2008 (Fig. 3) to be able to enhance the horizontal resolution over the urban area of Rome. The outer domain covers most of western Mediterranean area, centered at 41.5°N, 10.0°E with 27 km spatial resolution (D01 in Fig. 3). The nested domains cover Central Italy with a spatial resolution of 9 km for domain 2, 3 km for domain 3, and 1 km for the innermost domain (D04 in Fig. 3). D04 covers the city area and its surroundings (Lazio region) and it overlaps the ERS satellite swath.

The following model configuration has been used, based on previous studies and sensitivity test over the same area [19]:

1) 33 unequally spaced vertical sigma levels (σ), from the surface up to 100 hPa, with a higher resolution in the planetary boundary layer (PBL) than in the free atmosphere;
2) the medium-range forecast MRF scheme for the PBL. This scheme is based on the Troen-Mahrt representation of counter-gradient term and the eddy viscosity profile in the well-mixed PBL [20];

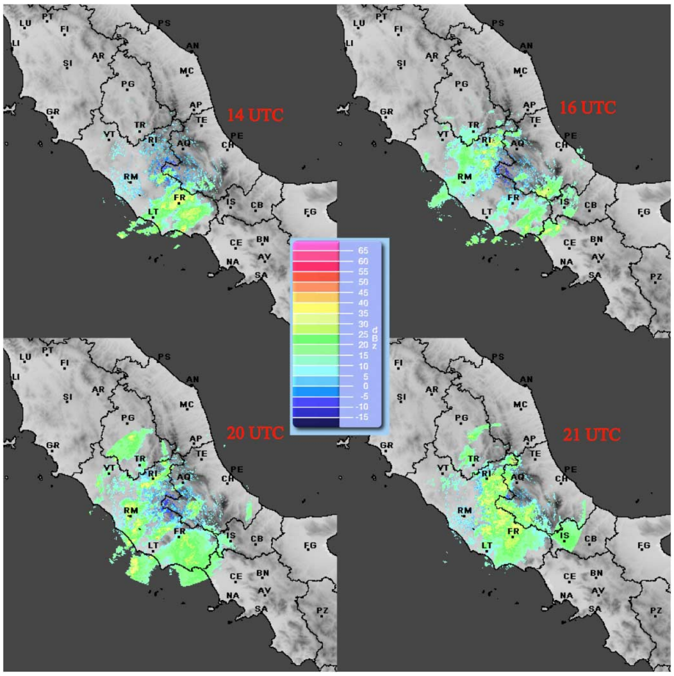

Fig. 2. Reflectivity maps on October 3, 2008 measured by the Doppler radar located over Midia Mountain (Central Italy), owned by the National Department of Civil Protection of Italy.

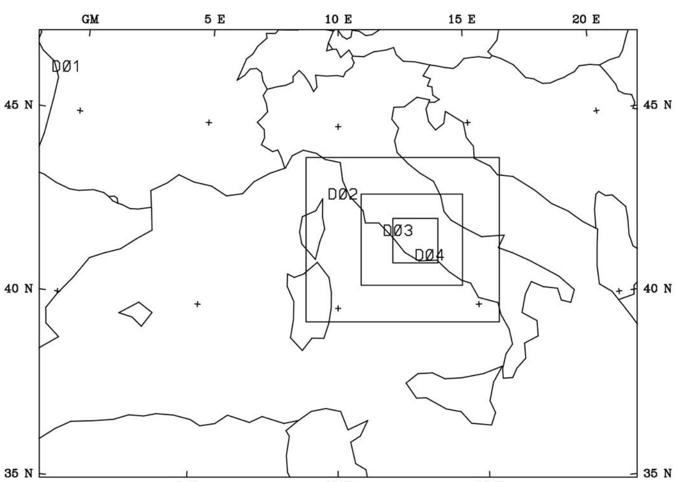

Fig. 3. MM5 domains configuration. Domain D01 has resolution of 27 km; D02 has resolution of 9 km; D03 has resolution of 3 km; and D04 has resolution of 1 km.

3) the CLOUD radiation scheme for radiative transfer processes. This scheme accounts for both shortwave and longwave interactions with explicit cloud and clear-air scattering [21];
4) the Kain-Fritsch-2 cumulus convection parameterization is used for domains 1 and 2 [22], [23], whereas no cumulus scheme is used for domains 3 and 4;
5) the Reisner-2 scheme for microphysics; based on mixed-phase scheme, graupel, and ice number concentration prediction equations [24].

The European Centre for Medium-Range Weather Forecast (ECMWF) analysis at 0.25° horizontal resolution for temperature, wind speed, relative humidity, and geopotential height is interpolated to the MM5 horizontal grid and to sigma levels to produce the model initial and boundary conditions.

B. InSAR Data Assimilation

The atmospheric data assimilation aims to incorporate observations into NWP models and to fill data gaps using physical, dynamical, and/or statistical information. Physical consistency, spatial and temporal coherence, and noise suppression are three of the major concerns in atmospheric data assimilation.

Briefly, the variational method is an optimization problem: 3DVAR attempts to find the best fit of a gridded representation of the state of the atmosphere (first guess or background field) to a discretely and irregularly distributed set of observations [25], [26]. The best fit is obtained by minimizing the so-called cost function $\mathbf{J}$, defined as

$$\boldsymbol{J} = \boldsymbol{J^b} + \boldsymbol{J^o} = \frac{1}{2}\left(\boldsymbol{x^b} - \boldsymbol{x}\right)^{\boldsymbol{T}} \boldsymbol{B}^{-1}\left(\boldsymbol{x^b} - \boldsymbol{x}\right) + \frac{1}{2}\left(\boldsymbol{y^o} - \boldsymbol{H}\left(\boldsymbol{x^b}\right)\right)^{\boldsymbol{T}} (\boldsymbol{E} + \boldsymbol{F})^{-1}\left(\boldsymbol{y^o} - \boldsymbol{H}\left(\boldsymbol{x^b}\right)\right) \quad (9)$$

where $\mathbf{x}^{\mathrm{b}}$ is the background term, $\mathbf{y}^{\mathrm{o}}$ is the generic observation, $\mathbf{H}(\mathbf{x}^{\mathrm{b}})$ is the corresponding value evaluated by the operator $\mathbf{H}$ used to transform the gridded analysis into the observation space. The solution of this equation $\mathbf{x} = \mathbf{x}^{\mathrm{a}}$ is the *a posteriori* maximum likelihood estimate of the true state of the atmosphere; $\mathbf{B}$, $\mathbf{E}$, and $\mathbf{F}$ are the covariance error matrices for the background, the observations, and the operator $\mathbf{H}$, respectively.

The 3DVAR is used to assimilate data of IWV, retrieved from InSAR and an external data source (MERIS) (as described in Section II), with the aim of improving ICs for MM5 [27].

Four interferometric stacks of ASAR images, acquired by the C-band radar aboard the European Envisat satellite in standard Stripmap mode, with a single-look resolution of 9 by 6 m (slant by azimuth), and over a swath of about 100 km, have been processed using the PS technique to generate InSAR APSs. The one used in this study, formed by 10 images, was collected over Rome along the Envisat descending track 351.

The InSAR APS measurements of the atmospheric path delay can be assumed similar to data provided by a dense GPS receivers network, thus the $\mathbf{H}$ operator implemented for GPS [28], [29] has been adopted in (9).

The descending SAR overpass was acquired at 0930 UTC on October 3, 2008, therefore a background analysis ($\mathbf{x}^{\mathrm{b}}$) is necessary at that time to assimilate the related APS data. Standard ECMWF analysis usually used to initialize model simulations is available every 6 h at synoptic times (e.g., 06 or 12 UTC), far away from the SAR overpass. A short-term MM5 simulation starting at 06 UTC of October 3 and ending at 09 UTC of the same day has been produced; the output at 09 UTC has been fed back to MM5 to be used as first guess for the 3DVAR. This procedure allows for having ICs at 09 UTC to initialize the forecast with assimilated InSAR data (MM5_VAR). Similarly, IC without assimilation of InSAR data is produced to perform a control run (MM5_NOVAR). No change of the atmosphere conditions is assumed between 09 UTC and 0930 UTC in order to use the ENVISAT data acquired at 0930 UTC (hypothesis of *frozen atmosphere*).

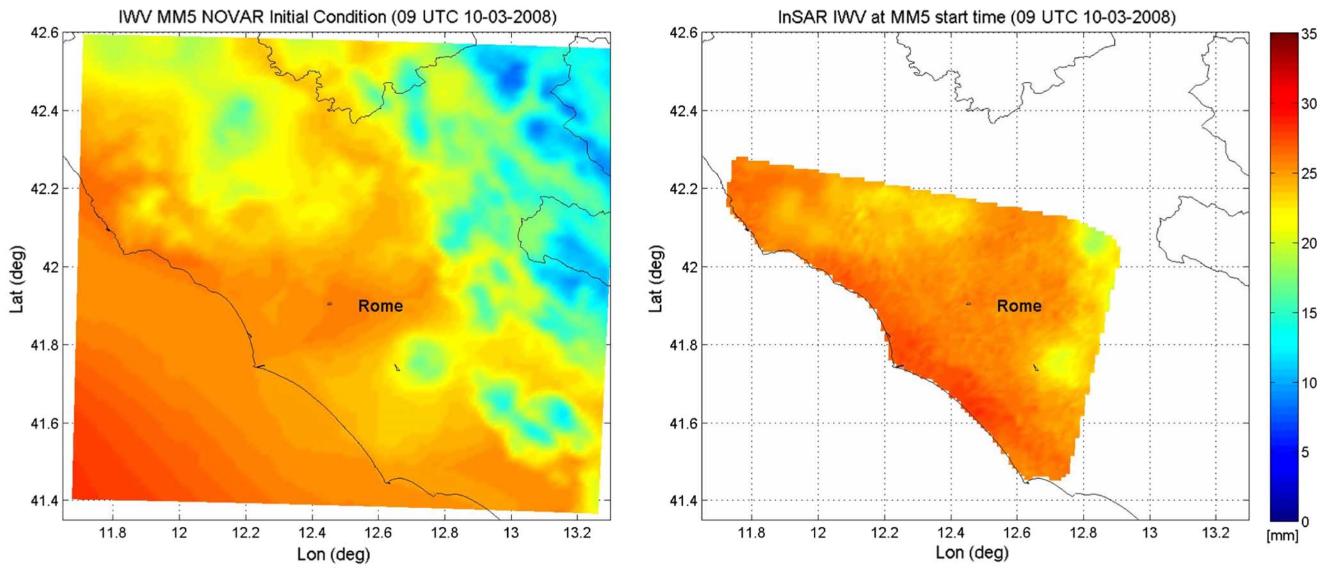

Fig. 4. Integrated water vapor at simulation start time (00 UTC of October 3, 2008) by MM5_NOVAR (left panel) and by InSAR down-sampled at the model grid resolution (right panel).

Moreover, a background ($\mathbf{B}$) and an observation error matrix ($\mathbf{E}$) need to be defined, as shown in (9). The $\mathbf{B}$ matrix is related to the climatology of the event and it is calculated on the whole month of October. To compute the $\mathbf{B}$ matrix, the "NMC method" is commonly used for NWP models [30], [31], where the forecast error covariance is calculated by using forecast difference statistics (e.g., differences between forecasts at $\mathrm{T}+48$ and at $\mathrm{T}+24$). The $\mathbf{E}$ matrix is built based upon the assumptions of 1) a constant IWV error estimated within $\sigma_{\mathrm{APS}} = 0.05$ cm [see (5)], which corresponds to a random error on the InSAR phase of the order of 15°, and 2) no cross correlation of observation errors between adjacent pixels. To make condition 2) as true as possible, a thinning of the observations is performed. Cardinali *et al.* [32] demonstrated that the influence of the assimilated data in the variational assimilation process is lower in data-rich areas and that a large error correlation among them decreases the observation influence in the assimilation process, increasing the weight of the background field [32]. Thus, the whole set of InSAR data has been down-sampled to the resolution of the innermost domain (1 km): for each MM5 grid point, the nearest available InSAR measurement is retained. An alternative to the thinning process would be an iterative cycle of assimilation which would allow to get only a portion of data at each assimilation cycle [32], but this method will be considered for future work.

V. Results of the Data Assimilation Experiment

A. Impact on ICs

The assimilation procedure of any meteorological field requires the adjustment of the other input variables (temperature, pressure, winds, etc.) in order to be coherent with the changes deriving from 3DVAR on the assimilated field. Fig. 4 shows the IWV field at MM5 start time when no assimilation is performed (MM5_NOVAR, left panel) and the IWV retrieved from InSAR data after thinning process and successively assimilated into the model IC (right panel). The InSAR data show a larger variability than MM5 in the same area and moister conditions along the Tiber Valley around Rome toward the coastline.

The impact of the water vapor assimilation on the IC can be evaluated by analyzing the increments with respect to the background field. An example is given in Fig. 5, showing the water vapor mixing ratio (QVP, left panel) and the ground temperature (TGK, right panel) increments over MM5 innermost domain at the start time (09 UTC).

The QVP increments (Fig. 5, left panel) clearly show that changes occur in the area where the InSAR data are available, whereas the temperature adjustments (Fig. 5, right panel) are spread all over the domain. The increments of QVP range from 0% to around the 4% of the first guess field (MM5_NOVAR), whereas surface temperature increments rise up to a maximum of 6%.

An assimilation experiment with MERIS data within the Envisat swath (MM5_ME) was also performed (not shown) to evaluate their impact on the final results, as MERIS has been used for IWV retrieval from InSAR data (Section II). It was found that mainly negative increments are produced by MERIS assimilation on QVP field; also in this case, increments are nonzero only where MERIS data are available. At the start time, the IWV of the MM5_VAR simulation shows a larger spatial variability than MM5_ME and an IWV increase close to the coastline that is not present on MM5_ME. A comparison of MM5_ME with observations, analogous to the one that is presented in the following sections, shows profiles similar to those produced by InSAR assimilation but with larger biases for most of the variables. On the other hand, the comparison shows a negligible impact on the precipitation field. This implies that the enhanced spatial variability introduced by the InSAR is crucial to produce changes that will be discussed below. A deeper investigation of these results would be necessary, but they are sufficient to ascribe the improvements found

Thisarticlehasbeenacceptedforinclusioninafutureissueofthisjournal.Contentisfinalaspresented,withtheexceptionofpagination.

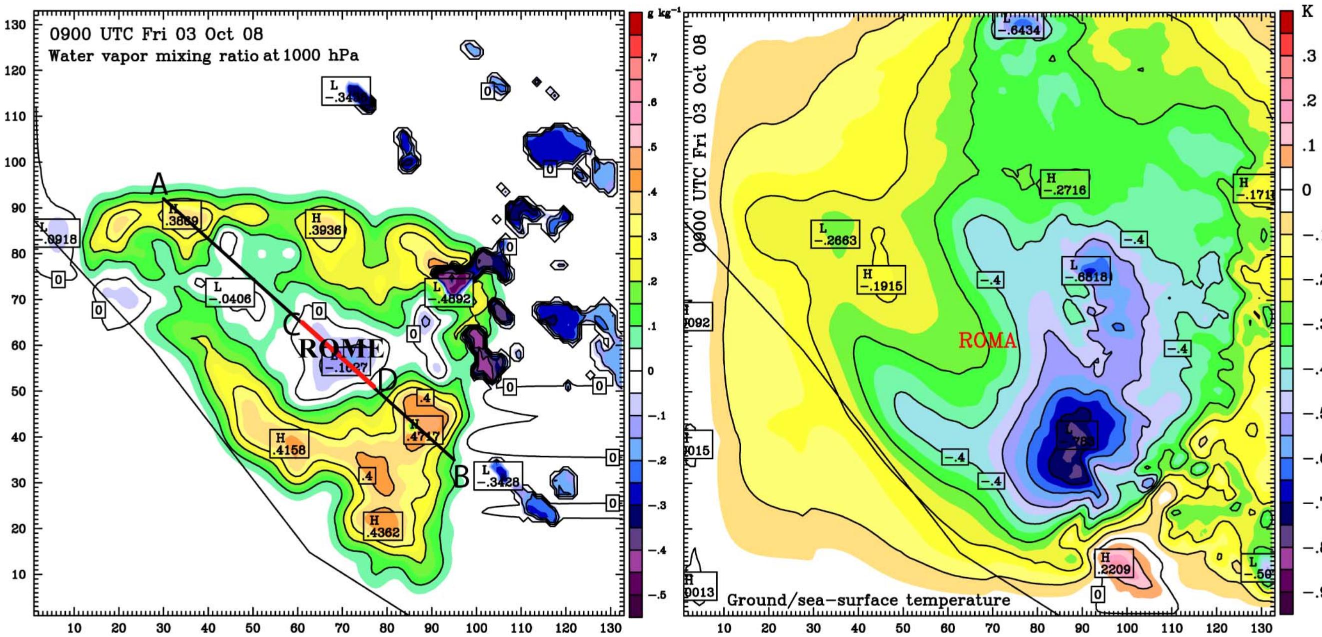

Fig. 5. Increment of water vapor mixing ratio (g/kg) at 1000 hPa (left panel) pressure level and of the ground temperature (K, right panel) at start time 09 UTC on the highest resolution domain of MM5 model after InSAR data assimilation. AB (black) and CD (red) are two cross-sectional lines.

for MM5_SAR mainly to the InSAR data assimilation, as discussed later.

B. Vertical Structure: Water Vapor and Soundings

As a first assessment of the impact of InSAR assimilation, a comparison of the vertical distribution of water vapor at the lower atmospheric layers between the two simulations (MM5_NOVAR and MM5_VAR) has been performed. A vertical cross section centered in Rome and crossing the InSAR swath (Fig. 5, line AB) on MM5 domain 4 shows that the largest differences between MM5_NOVAR and MM5_VAR simulations are seen within 3 h from the start time, whereas they are negligible after 12 UTC. Between 09 UTC and 10 UTC, the two simulations show differences both in the vertical content of water vapor and in its horizontal variability (Figs. 6 and 7), whereas only small differences on its content are found in the following hours. Fig. 6 shows the cross section at 09 UTC of October 3 for the two simulations (MM5_NOVAR on the left and MM5_VAR on the right); the assimilation of InSAR data (right panel) causes both a reduction of the vapor content and a cooling of the layers: the 9.6 g/kg contour, e.g., reaches 750 m instead of 830 m as for MM5_NOVAR.

These characteristics are found all along the vertical cross section. By 10 UTC, changes in the vertical section are found especially across the urban area of Rome (area inside the two gray dashed lines in Fig. 7). A few differences are found also above 1 km for both the water vapor and the thermal structure, and will be discussed later.

This first comparison allows to assess an impact of the assimilation on the evolution of the atmospheric conditions, but a further and more objective comparison with experimental data is performed to evaluate its effectiveness.

A comparison between model results and radio-sounding observations (RAOB) is performed to investigate the InSAR data impact on the profiles of temperature (T), water vapor mixing ratio (QVP), and wind (WSP for speed and WDR for direction). The comparison is shown in Fig. 8 where also the bias (defined as difference between observation and model) for all variables has been computed.

Soundings launched from the center of Rome (41.90°N, 12.52°E) during the METAWAVE campaign and from Pratica di Mare (41.65°N, 12.43°E) are used; the model results are interpolated at the sites' coordinates for the comparison. The main differences between the two simulations in the site of Pratica di Mare are found at the start time, but no experimental data are available at that time (09 UTC). At 12 UTC, the two MM5 profiles (MM5_NOVAR and MM5_VAR) are very similar (not shown) and no appreciable difference is detectable for this site.

Two soundings are available over Rome at 10 UTC and 1230 UTC. The profile at 10 UTC (Fig. 8, top left panel) shows that the model overestimates the observed water vapor (gray line) near the surface, with MM5_VAR (black solid line) producing larger bias (correspondent black solid line on the left) than MM5_NOVAR (black dashed line): an overestimation of approximately 1.0 g/kg (MM5_VAR) and 0.20 g/kg (MM5_NOVAR) is produced at 80 m of height. At higher levels, between 150 m and 1000 m, the two simulations show opposite results: MM5_NOVAR (black dashed line) produces an underestimation, whereas MM5_VAR (black solid line) an overestimation, but with a smaller bias than the control run. Correspondingly, a cooling of the layer is detected for MM5_VAR simulation (Fig. 8, black solid line on the top right panel) with a larger bias with respect to the observations (at 80 m level the bias increases from 1.1 °C of MM5_NOVAR to 1.8 °C of MM5_VAR). Even if MM5_VAR

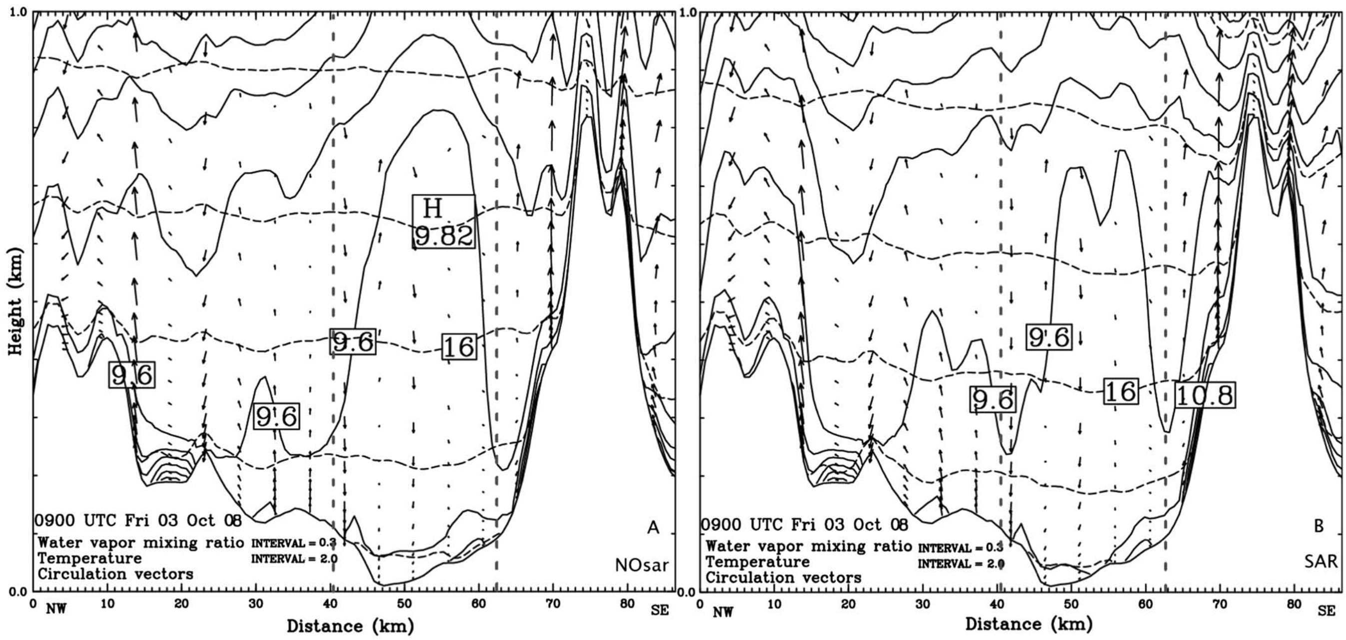

Fig. 6. Water vapor mixing ratio (g/kg, solid line), temperature (°C, dashed lines), wind vectors on a vertical cross section taken over the InSAR swath (line AB of Fig. 5) at 09 UTC of October 3rd (start time). The area inside the two vertical gray dashed-lines represents a portion of the section over the urban area of Rome (line CD of Fig. 5). The two panels refer respectively to the control run MM5-NOVAR (left) and the assimilated one MM5-VAR (right).

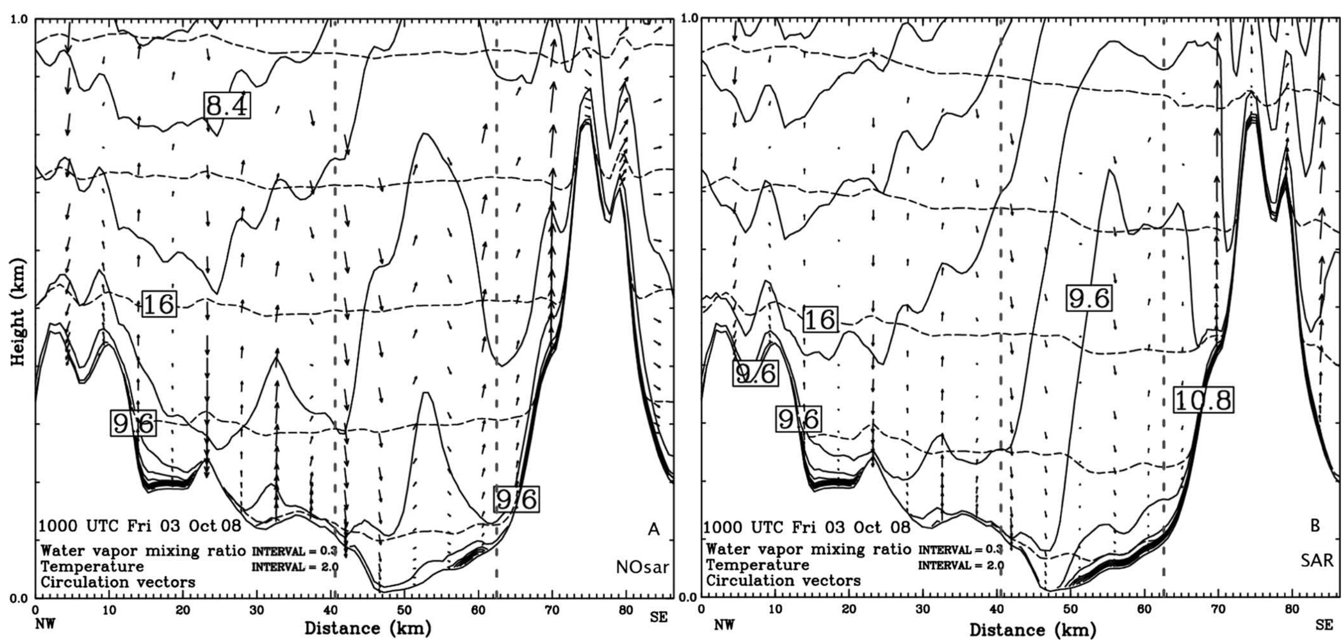

Fig. 7. Water vapor mixing ratio (g/kg, solid line), temperature (°C, dashed lines), wind vectors on a vertical cross section taken over the InSAR swath (line AB of Fig. 5) at 10 UTC of October 3rd. The area inside the two vertical gray dashed-lines represents a portion of the section over the urban area of Rome (line CD of Fig. 5). The two panels refer respectively to the control run MM5-NOVAR (left) and the assimilated one MM5-VAR (right).

(Fig. 8 top right, black solid line) shows a higher temperature than MM5_NOVAR (black dashed line) near the surface, it shows a larger lapse rate than MM5_NOVAR within the first 50 m, resulting into an excessive cooling of the upper layers. Above 1 km, both the simulations tend to overestimate the observed water vapor (Fig. 8, top left panel) and only negligible differences are found between the two temperature profiles (Fig. 8, top right panel). On the other hand, a positive impact of the InSAR assimilation is detected on the wind fields (Fig. 8, bottom panels) with a reduction of wind speed between 80 and 1000 m height for the MM5_VAR simulation (black solid line). This reduces the bias (correspondent black solid line on the left): at 500 m, for example, a bias reduction of 0.7 m/s is found. The wind direction profiles for the two simulations are very similar (Fig. 8, bottom right panel), but with a more marked south component of the south-westerly flow below 250 m resulting from MM5_VAR (black solid line) than from MM5_NOVAR (black dashed line). This turns into

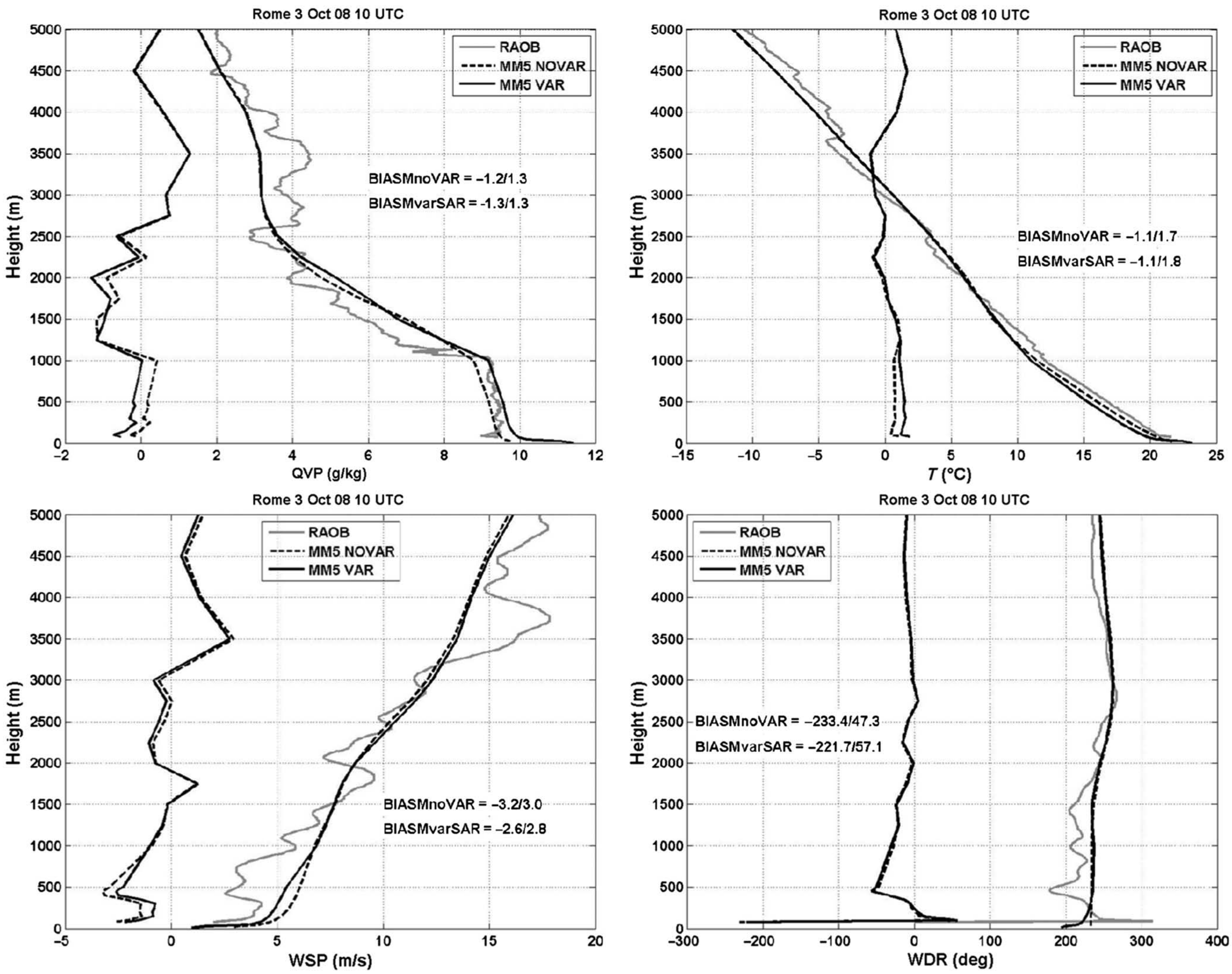

Fig. 8. Comparison between radio-soundings (gray lines) and model result (black dashed lines for MM5_NOVAR with its correspondent bias on the left, black solid lines for MM5_VAR with its correspondent bias on the left) for water vapor mixing ratio (top left), temperature (top right), wind speed (bottom left) and wind direction (bottom right) in Rome (41.90°N, 12.52°E) at 10 UTC of October 3rd, 2008. Biases are calculated between observed and simulated data. For each panel the minimum/maximum bias along the profile is indicated for the two simulations.

an enhanced advection of humid air, partially explaining the moister atmosphere at the lowest levels for this simulation.

Fig. 9 shows the vertical profiles over Rome at 1230 UTC: small differences are found between MM5_NOVAR (black dashed lines) and MM5_VAR (black solid line). At this time, the InSAR data assimilation tends to reduce the bias for most variables. The mixing ratio vertical profiles show an overestimation for both MM5_NOVAR and MM5_VAR (Fig. 9, top left panel black dashed and black solid lines, respectively) with respect to radiosonde data below 1 km (bias ∼1.3–2.6 g/kg), with a very small reduction of the error below 750 m when InSAR data are assimilated (black solid lines). Between 1.5 and 3.5 km, MM5_VAR (black solid line) tends to reproduce a smoothed profile, close to the mean of the observed profile (gray line), reducing the bias; on the other hand, the control simulation (black dashed line) continues to overestimate RAOB data.

Differences between MM5_NOVAR and MM5_VAR on the temperature profiles (Fig. 9, top right panel, black dashed and black solid lines, respectively) are small, even if reduced errors are found when InSAR data are assimilated (black solid line). This is especially true in the layer between 1.5 and 2.5 km, where the maximum bias with respect to the observations decreases from 1.3 to 0.5 °C. This small reduction of the biases for both QVP and T produced by the InSAR data assimilation improves the relative humidity profile with a reduction up to 5% of the bias with respect to RAOB data below 1 km, and on average up to 10% above (between 1.5 and 3.0 km). The improvements produced by the InSAR data assimilation on the water vapor content can partially be related to the correction of the advection highlighted by the comparison between the wind fields of the two simulations. The wind speed profile for MM5_VAR (Fig. 9, bottom left panel, black solid line) shows a reduction of both the overestimation with respect to the radiosounding (gray line) below 2 km (mean bias decreases from 2.4 m/s for MM5_NOVAR to 1.2 m/s for MM5_VAR) and of the underestimation between 2 and 3 km (mean bias decreases from 1.3 m/s for MM5_NOVAR to 0.2 m/s for MM5_VAR).

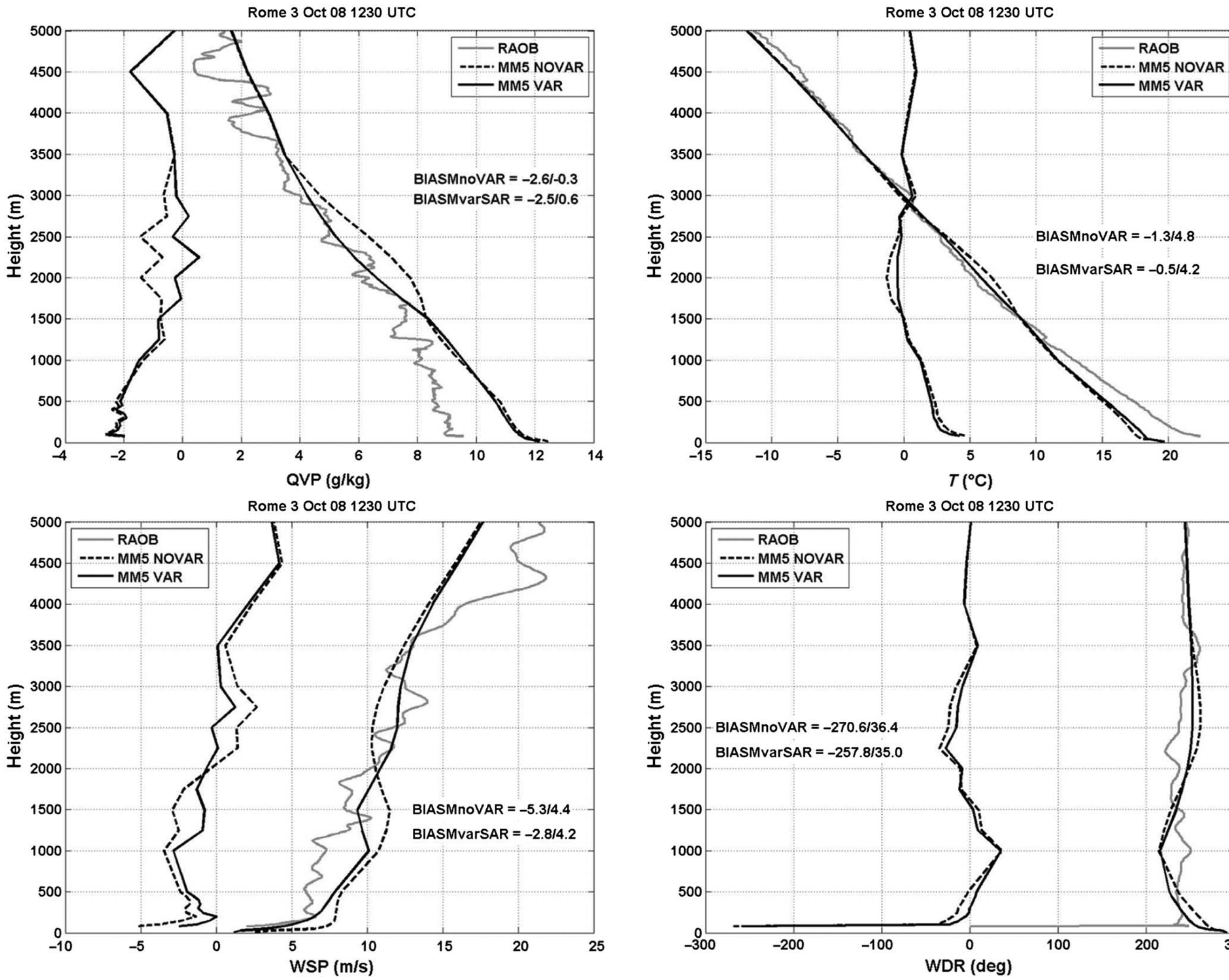

Fig. 9. Comparison between radio-soundings (gray lines) and model result (black dashed lines for MM5_NOVAR with its correspondent bias on the left, black solid lines for MM5_VAR with its correspondent bias on the left) for water vapor mixing ratio (top left), temperature (top right), wind speed (bottom left) and wind direction (bottom right) in Rome (41.90°N, 12.52°E) at 1230 UTC of October 3rd, 2008. Biases are calculated between observed and simulated data. For each panel the minimum/maximum bias along the profile is indicated for the two simulations.

The differences of the wind direction between MM5_NOVAR and MM5_VAR (Fig. 9, bottom right panel, black dashed and black solid lines, respectively) are small, even if also in this case, the InSAR data assimilation turns into a small reduction of the bias with respect to measurements (gray line): on average from 23° for MM5_NOVAR (black dashed lines) to 15 degrees for MM5_VAR (black solid lines).

In spite of an enhancement of the error close to the start time (10 UTC) for both the temperature and the water vapor mixing ratio profiles near the surface, the results show an improvement of the dynamical fields that might contribute to the more correct evolution of the system verified with the comparison of profiles at 1230 UTC (Fig. 9). This allows us to conclude that there is a better agreement between the assimilated simulation and the observations than for the control run in terms of thermodynamical variables. Accordingly, a positive impact of the assimilation also on the precipitation forecast can be hypothesized.

C. *Precipitation Forecast*

To assess the impact of the InSAR data assimilation on the rain forecast, a comparison with the observed precipitation field is carried out. The rain retrieved from the Mount Midia radar (Fig. 10) is available from the Civil Protection Department of the Abruzzo Region [33], [34]. The radar shows rain starting offshore at 12 UTC and moving inland at 13 UTC (not shown). Fig. 10 shows that the 3-h accumulated rain has a pattern aligned along a northeast-southwest axis (NE-SW) for most of the time. Until 15 UTC (Fig. 10, top left panel), weak to moderate rain is detected in the southeast of Lazio: a wide area of rainfall is shown northwest of the city of Frosinone (FR), extending up to the coast (up to 12 mm/3 h); very localized cells are observed on the east side of Rome (RM), with rain reaching 18–20 mm/3 h (actually accumulated in 1 h between 13 and 14 UTC). In the following 3 h (Fig. 10, top right panel), most of the Lazio region is interested by weak precipitation, with intense rainfall on the east side of Rome. Two

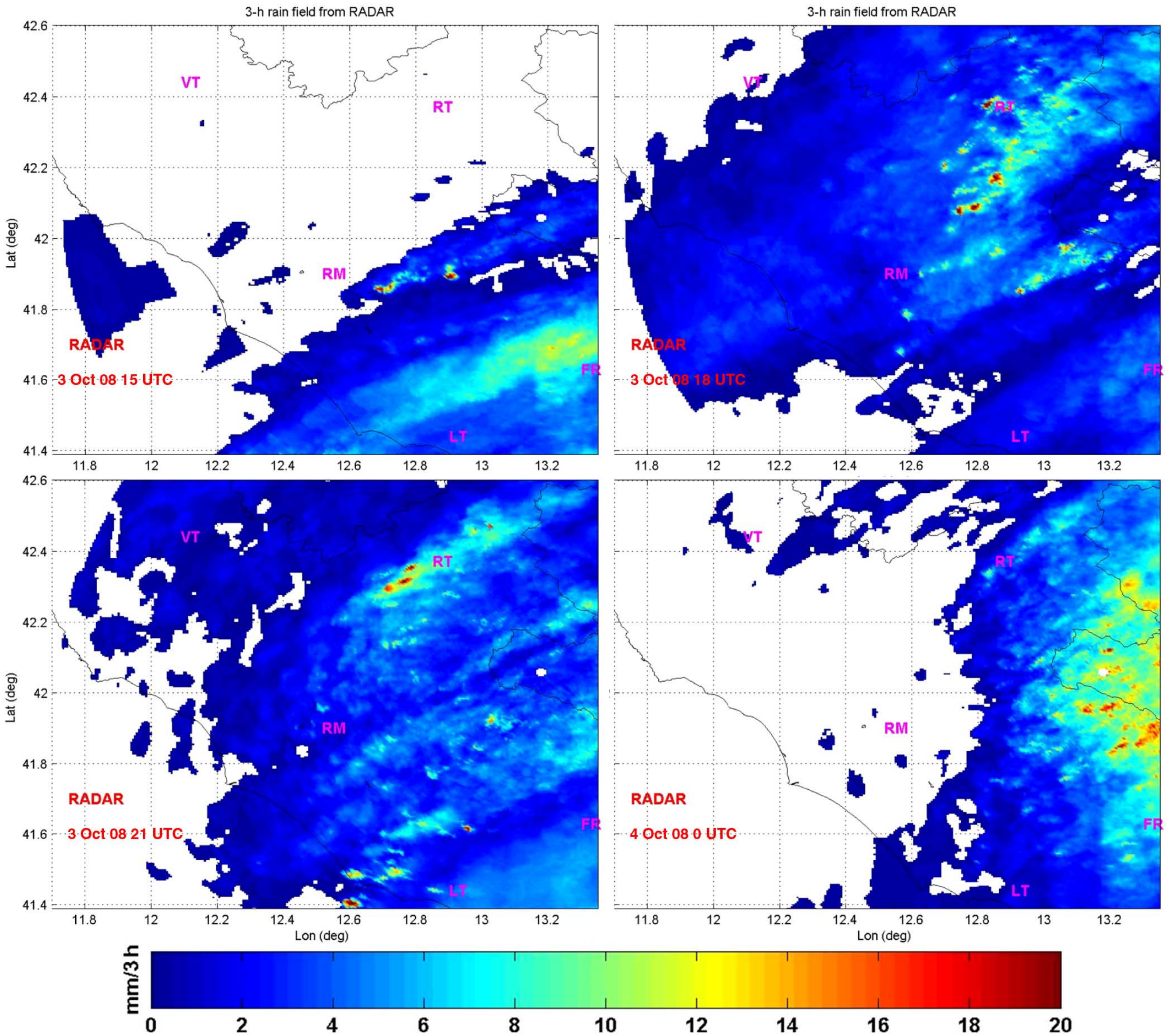

Fig. 10. Observed 3 h rainfall estimated from Abruzzo Region Radar on Mount Midia (42.05°N, 13.17°E) ending at 15 UTC (top left), 18 UTC (top right), 21 UTC (bottom left), 24UCT (bottom right) of October 3, 2008 over Lazio and west Abruzzo regions. Main cities of the region are indicated in pink: Rome (RM), Rieti (RT), Viterbo (VT), Latina (LT), and Frosinone (FR).

structures are detected also at this time: the first one south of Rieti (RT) with rain from 8 to 20 mm/3 h, whereas the second one reaching 18 mm/3 h with localized maxima east of Rome (also in this case, the precipitation occurred during the last hour).

During the 3 h period ending at 21 UTC, the precipitation is spread over most of Lazio region with intense rain rates on the east and southeast (Fig. 10, bottom left panel); hourly maps (not shown) show diffuse (3–8 mm/h) in the area around Rieti (RT) with more intense cells developing at 20 UTC (12–18 mm/h) south-east of the city. Weak precipitation (8 mm/3 h) is measured in the area between Frosinone (FR) and Latina (LT), whereas spread rain falls between 20 UTC and 21 UTC on the east side of Rome (6–10 mm/h). After 21 UTC (Fig. 10, bottom right panel), the rain moves eastward, mainly affecting the border territories between Lazio and Abruzzo, with heavy rain occurring between 21 UTC and 22 UTC (8–12 mm/h); rain ended by midnight.

A similar rain field is found for MM5_NOVAR (Fig. 11) and MM5_VAR (Fig. 12). No influence of the InSAR data assimilation is found on the timing of the event: in both cases, MM5 forecasts precipitation starting after 11 UTC with very weak rain rates on the east side of Rome, earlier with respect to the Radar observations. An intensification of the rain is produced after 14 UTC. MM5 correctly reproduces the NE-SW axis of the rain structures, yet highlighted by the Radar measurements.

Both simulations (MM5_NOVAR and MM5_VAR) forecast the precipitation in the Rieti district (RT) earlier than the observations (before 15 UTC, Figs. 11 and 12, top left panels). In the 3-h interval ending at 15 UTC, MM5 correctly reproduces two areas of maximum precipitation [(Fig. 10, east of Rome and between Latina (LT) and Frosinone (FR)], in good agreement

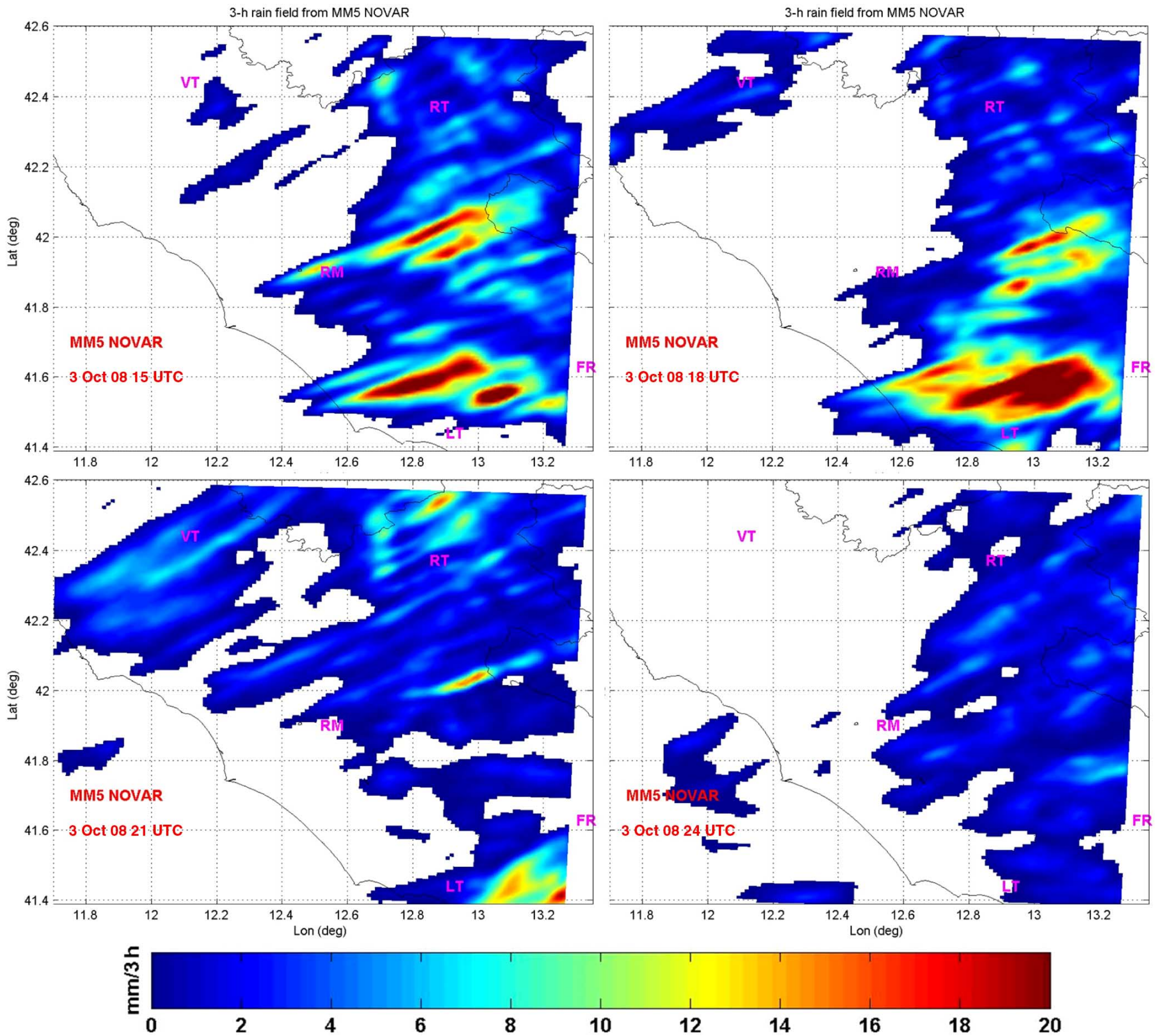

Fig. 11. MM5 simulated 3-h rainfall without assimilation (MM5_NOVAR) ending at 15 UTC (top left), 18 UTC (top right), 21 UTC (bottom left), 24UCT (bottom right) of October 3, 2008 over Lazio and west Abruzzo regions.

with the radar, but with a displacement with respect to the observations. The MM5_VAR simulation shows the first maximum more widespread than MM5_NOVAR and it produces a larger overestimation with respect to the radar (the bias increases of about 8 mm/3 h).

The model reproduces the precipitation structure between LT and FR (Figs. 11 and 12, top left panel) with a westward extension with respect to the radar (Fig. 10, top left panel). Both simulations overestimate the rainfall (Figs. 11 and 12, top left panels). The InSAR data assimilation partially corrects the rain intensity: the overestimation is reduced on the west side of the precipitation area of about 8 mm/3 h with a more realistic west-east rain intensity gradient.

In the following 3 h (Figs. 11 and 12, top right panels), both MM5 simulations continue to produce weak rain over Rieti (RT) district, showing a system of localized cells in partial agreement with the radar (Fig. 10, top right panel), but none of them correctly reproduces the highest intensities. MM5_VAR (Fig. 12, top right panel) shows a small intensification of the cells, slightly reducing the error with respect to the observed field. In order to explain the MM5 underestimation over Rieti (RT) of the precipitation in this time interval (15–18 UTC), one can speculate that the early onset of the precipitation by MM5 in this area excessively depletes the water vapor available for rain formation during the following hours. The InSAR assimilation at start time is not sufficient to fully correct this error in a few hours.

At this time (15–18 UTC), both model runs show a maximum precipitation east of Rome (Figs. 11 and 12, top right panels). Also in this case, there is a good agreement between the model and the radar in terms of maxima values, but MM5 produces heavy rain on a wider area than that observed; MM5_VAR,

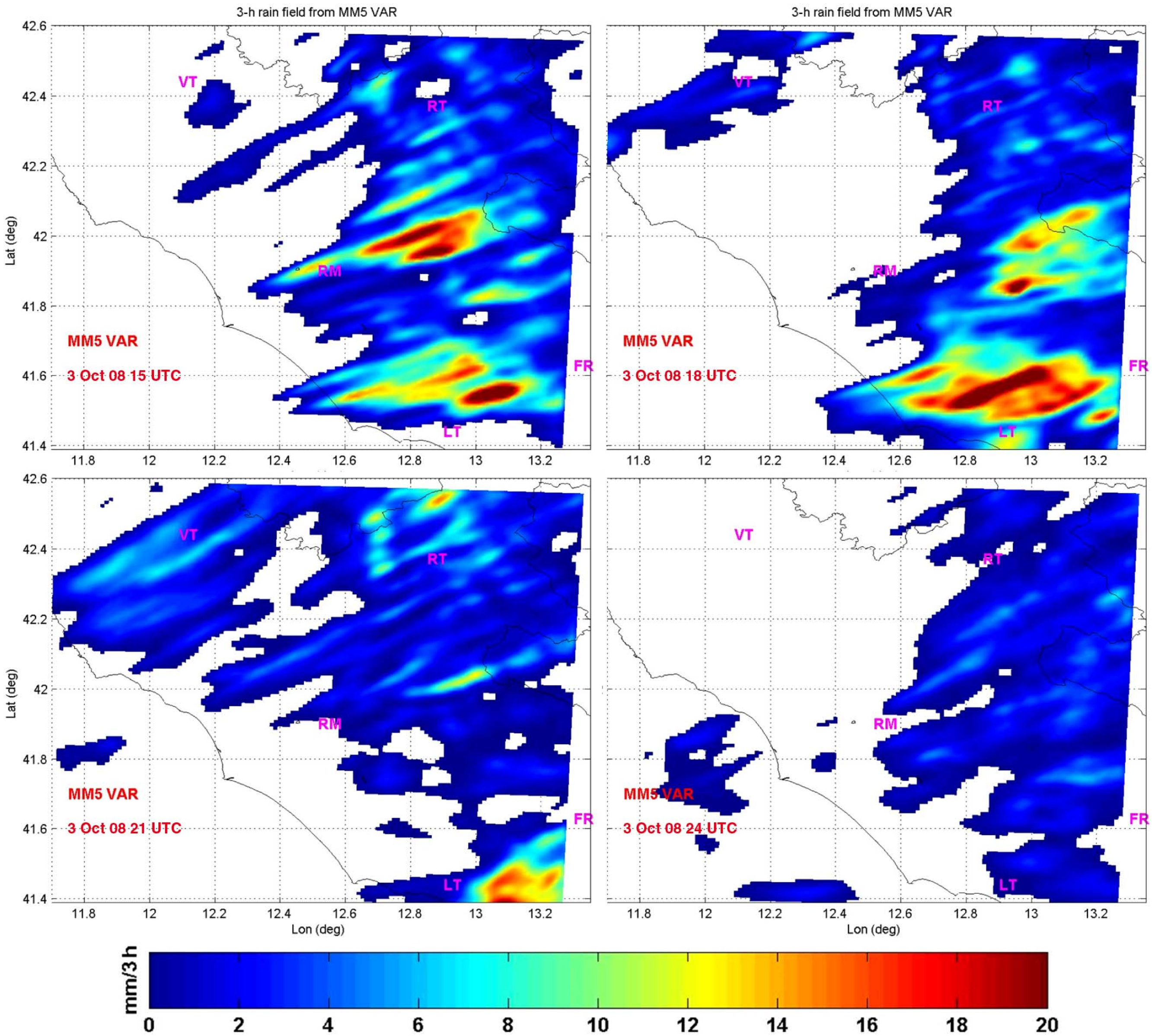

Fig. 12. MM5 simulated 3-h rainfall with InSAR-integrated water vapor assimilation (MM5_VAR) ending at 15 UTC (top left), 18 UTC (top right), 21 UTC (bottom left), 24UCT (bottom right) of October 3, 2008 over Lazio and west Abruzzo regions.

moreover, tends to further spread the precipitation, worsening the agreement with the observations (Fig. 12). In addition, the model continues to produce heavy precipitation in the southern part of the domain, largely overestimating the radar in the same area; in this case, the InSAR data assimilation seems to have an effect on reducing the rain accumulation and the discrepancy with the measurements. However, the area of maximum precipitation is too wide also in the MM5_VAR simulation.

During the successive 3 h ending at 21 UTC (Figs. 11 and 12, bottom left panels), both the simulations correctly produce rain over the Viterbo area (VT), slightly overestimating the rain retrieved by the radar. At 20 UTC, the model correctly simulates the development of a few cells near Rieti (RT), with a spatial shift of the structure. The MM5_VAR simulation (Fig. 12, bottom left panel) does not correct the spatial displacement of the cells, but it increases the rate of the southwest cells while decreases that on the northwest side, thus partially increasing the agreement with the radar observations. A further small correction is produced by MM5_VAR reducing the rate of the cell simulated east of Rome (Figs. 11 and 12, bottom left panels). On the other hand, MM5 overestimates the precipitation on the bottom right corner of the domain by few mm/3 h up to about 9 mm/3 h for MM5_NOVAR, to about 11 mm/3 h for MM5_VAR.

After 21 UTC (Figs. 11 and 12, bottom right panels), only weak rain is produced by the model, regardless of the assimilation process, causing a large bias with respect to the radar, partially reduced in the MM5_VAR simulation by roughly 3 mm/3 h.

The results suggest that the assimilation of IWV data retrieved from InSAR has an impact on the precipitation forecast, but it is not always positive. The positive impact occurs when the rain structures develop during a time interval longer than half an hour and spread over wide areas at a horizontal

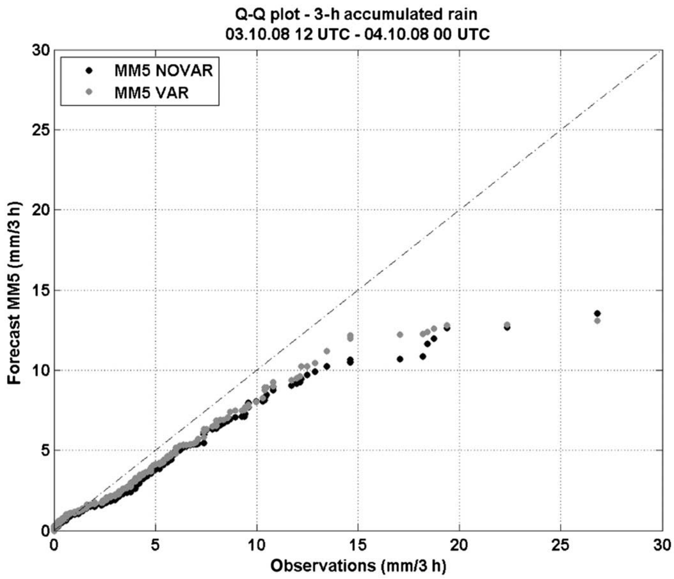

Fig. 13. Q–Q plot of the 3h accumulated precipitation for October 3rd, 2008 in the time interval between 12 and 24 UTC. Observed and forecasted quantile thresholds are respectively on the x and y axes. Control simulation (MM5_NOVAR) is represented in black and assimilated one (MM5_VAR) in gray.

scale comparable to or larger than that of the model. On the other hand, it fails in correcting the field, or it has even a negative impact, on very localized precipitation (model subgrid scale). The assimilation in terms of IWV, which is a 2-D field, has limits in correcting the model dynamics. Significant improvements on the rain field would be probably achievable if water vapor data were assimilated together with wind data [1], [31], [35]. An experiment in this sense would be very interesting and would probably correct at least the space bias of the rain field; it is beyond the aim of this study but it represents a challenging future step.

VI. Statistics

To evaluate the impact of the assimilation of InSAR data, a few statistical methods and indices commonly used for weather forecasting are applied in this section: the quantile-quantile (QQ) plot, the Equitable Threat Score (ETS), and the frequency bias (FBIAS) [36]. The QQ plot is a graphical method to compare the distribution of forecast and observation; data are sorted from smallest to largest and their percentile values are compared. The ETS roughly quantifies the percentage of correct forecasted rainy events that can be related to the model skill (i.e., the percentage of nonrandom correct forecasts), with values ranging from slightly negative (forecast worse than random) to 1 (perfect forecast). The FBIAS score allows for evaluating the frequency of the total forecasted events (hits and false alarms) at a given threshold values, e.g., a value above/below 1 indicating an over-/under-forecasted event.

The MM5 results are compared with observations from the rain gauge network of the Italian Civil Protection Department (DPC) over Lazio and Abruzzo; the 145 gauges that were available within the D04 domain are used for the comparison. Fig. 13 shows the QQ plot of the 3-h accumulated rain for the two simulations (MM5_NOVAR in black and MM5_VAR in gray) with respect to the observations. MM5 produces an underestimation of precipitation events for threshold above 3 mm/3 h regardless of the assimilation process; the underestimation increases for medium-high threshold (>15 mm$/3$ h). It is worth noting that the assimilation of the IWV retrieved from InSAR reduces the underestimation, especially in the interval between 12 and 20 mm/3 h.

The ETS is computed for 12-h accumulated rain between 21 and 24 UTC of October 3 (every 3 h), with the goal of partially reducing the negative impact of the time bias of the event evolution. The ETS index increases from 0.16, 0.19, and 0.20 for MM5_NOVAR to 0.23, 0.22, and 0.23 for MM5_VAR, respectively, for the threshold values of 1, 3, and 6 mm. Moreover, MM5_VAR produces a higher score than MM5_NOVAR up to the threshold of 9 mm; for intermediate thresholds (10–15 mm), the ETS decreases and differences between the two simulations become negligible above 15 mm.

These results highlight that the InSAR assimilation has an impact on the forecast, with some improvements at weak precipitation thresholds. This is confirmed by the FBIAS computation for the 12-h accumulated rain: the MM5_VAR simulation shows an index higher than MM5_NOVAR for thresholds up to 12 mm/12 h; mean FBIAS increases from 0.64 to 0.74 within that threshold limit. This means that the water vapor assimilation reduces the underestimation of the frequency of events that affects the model for low to moderate rainfall. It is worth noting that both the ETS and FBIAS computed for shorter accumulation intervals (3 h) give similar results but produce lower scores, as expected.

VII. Summary and Conclusion

This paper presents an experiment aimed at exploiting the APS maps, provided by a multipass interferometric processing of SAR images, for the purpose of weather prediction. In particular, the IWV map retrieved from ASAR multipass interferometric data and MERIS products has been assimilated into the mesoscale numerical prediction model MM5.

The experiment is carried out in the framework of the ESA METAWAVE project, as the final step of a comprehensive study for evaluating the water vapor path delay through the atmosphere and its mitigation in SAR interferometry applications. In this frame, the InSAR comes out as a potential candidate to provide valuable information about high-resolution water vapor field. The correct estimation of the water vapor into the weather forecast IC is one of the most important factors for a good forecast. A support from an external source (in this study a sequence of MERIS water vapor products) is necessary to turn the differential APS information into an absolute estimate of the tropospheric path delay. Once obtained, the high-resolution water vapor field, the data were thinned to the NWP model resolution and assimilated using a three-dimensional (3-D) variational technique. The impact of this assimilation on the forecast is investigated by analyzing both direct and indirect effects.

The detected differences on vertical sections of the atmosphere between the control run (MM5_NOVAR) and the simulation with assimilated InSAR data (MM5_VAR) have highlighted an impact of the InSAR assimilation on the model vertical distribution of the water vapor, especially until few hours right after the start time. The assimilation changes the thermodynamical structure of the atmosphere and it introduces a larger vertical variability of the water vapor field. The comparison between the vertical profiles of water vapor mixing ratio, temperature, and wind field shows the impact of the SAR assimilation on the thermodynamical structure. It shows differences between the control and assimilated simulations on the site of Rome: despite an increase of the error by the assimilated run on the water vapor content and temperature at lower levels close to the start time, a remarkable correction of the wind field is produced by the assimilation at this time. This is supposed to contribute to a better forecast in the following hours, as shown by the comparison with a second sounding on the same site at a later time, showing a better agreement with the observations of the assimilated run than the control run for all variables.

Finally, the impact on the precipitation forecast has been evaluated. The model results are qualitatively compared with the rain field retrieved from a ground-based meteorological radar. This comparison shows no appreciable impact of the InSAR data assimilation on the temporal evolution of the event. A positive impact would likely require the assimilation of additional dynamical data (i.e., wind field) in the assimilation process.

On the other hand, impacts on the rain intensities are found: these are positive for precipitating structures extended over wide areas (larger than the model horizontal resolution scale) and developing on time intervals longer than half an hour, whereas it is negative for convective structures at subgrid scale. Moreover, the simulation with the InSAR data assimilation improves the forecasting performance of the spatial gradient of the rain, mainly, for systems with multiple cells. It is reasonable to suppose that this result could be improved by running simulations with resolution grid higher than 1 km, thus fully exploiting the high resolution of the APS maps of few hundred meters which, in principle, could provide a better description of very local phenomena.

A comparison between the forecasted precipitation with the measurements available from the Civil Protection Department rain gauge network over the region of interest allows to assess a general underestimation of the precipitation regardless of the assimilation of IWV, but it also highlights a reduction of this underestimation if InSAR data are used. The equitable threat score and frequency bias statistical indices have shown the difficulty of the model in correctly reproducing the moderate rain for this event, regardless of the InSAR vapor assimilation. However, the improvements shown by the InSAR assimilation for low precipitation thresholds (with a reduction of the model underestimation of the percentage of the total forecasted events and the increase in the number of the precipitating events correctly predicted) are encouraging for future developments.

This is the first study, to our knowledge, where differential atmospheric delay data derived by multipass SAR interferometric techniques are applied for weather prediction purposes. Although these results are preliminary, given that they are deduced from only one case study, they provide the potential of using the InSAR products in meteorological studies. The study results demonstrate that the IWV properly retrieved by InSAR can be useful for mesoscale assimilation and NWP. They allow assessing some impacts of the assimilation on the forecast, but they are not sufficient at the moment to support the hypothesis that such an impact is unequivocally positive for the precipitation forecast. The results should be generalized by adding more case studies. Other assimilation techniques could be tested to investigate the impact of the high resolved vapor data as provided by InSAR retrieval, as well as high-resolution simulations. Moreover, additional advantages derived from building optimal IC through InSAR data assimilation can be foreseen also by assimilating wind data from other sources.

Acknowledgment

The authors would like to thank all the METAWAVE participants for their valuable contribution and discussion; Abruzzo Region in Italy for providing radar data, E. Picciotti and F. S. Marzano for their helpful suggestions; Italian Civil Protection Department for providing rain gauges data; and University of Wyoming Department of Atmospheric Science for making available radio-soundings data on the Pratica di Mare site.

References

[1] Y.-H. Kuo, Y.-R. Guo, and E. Westwater, “Assimilation of precipitable water measurement into a mesoscale numerical model,” *Mon. Weather Rev.*, vol. 121, no. 4, pp. 1215–1238, Apr. 1993.

[2] Y.-H. Kuo, X. Zou, and Y.-R. Guo, “Variational assimilation of precipitable water using a nonhydrostatic mesoscale adjoint model. Part I: Moisture retrieval and sensitivity experiments,” *Mon. Weather Rev.*, vol. 124, no. 1, pp. 122–147, Jan. 1996.

[3] E. Pichelli *et al.*, “Water vapour distribution at urban scale using high-resolution numerical weather model and spaceborne SAR interferometric data,” *Nat. Hazards Earth Syst. Sci.*, vol. 10, no. 1, pp. 121–132, Jan. 2010.

[4] R. F. Hanssen, T. M. Weckwerth, H. A. Zebker, and R. Klees, “High-resolution water vapor mapping from interferometric radar measurements,” *Science*, vol. 283, no. 5406, pp. 1297–1299, Feb. 1999.

[5] G. Panegrossi, R. Ferretti, L. Pulvirenti, and N. Pierdicca, “Impact of ASAR soil moisture data on the MM5 precipitation forecast for the Tanaro flood event of April 2009,” *Nat. Hazards Earth Syst. Sci.*, vol. 11, no. 12, pp. 3135–3149, Dec. 2011.

[6] F. Rocca, “Modeling interferogram stacks,” *IEEE Trans. Geosci. Remote Sens.*, vol. 45, no. 10, pp. 3289–3299, Oct. 2007.

[7] P. Mateus, G. Nico, and J. Catalão, “Can spaceborne SAR interferometry be used to study the temporal evolution of PWV,” *Atmos. Res.*, vol. 119, no. SI, pp. 70–80, Jan. 2013.

[8] N. Pierdicca *et al.*, “Atmospheric water vapor effects on spaceborne interferometric SAR imaging: Comparison with groundbased measurements and meteorological model simulations at different scales,” in *Proc. IEEE Int. Geosci. Remote Sens. Symp. (IGARSS)*, 2009, vol. 5, pp. 320–323.

[9] S. Sahoo *et al.*, “3-D humidity retrieval using a network of compact microwave radiometers to correct for variations in wet tropospheric path delay in spaceborne interferometric SAR imagery,” *IEEE Trans. Geosci. Remote Sens.*, vol. 49, no. 9, pp. 3281–3290, Sep. 2011.

[10] S. Bonafoni, V. Mattioli, P. Basili, P. Ciotti, and N. Pierdicca, "Satellite-based retrieval of precipitable water vapor over land by using a neural-network approach," *IEEE Trans. Geosci. Remote Sens.*, vol. 49, no. 9, pp. 3236–3248, Sep. 2011.

[11] D. Cimini *et al.*, "On the accuracy of integrated water vapor observations and the potential for mitigating electromagnetic path delay error in InSAR," *Atmos. Meas. Tech.*, vol. 5, no. 5, pp. 1015–1030, May 2012.

[12] M. Montopoli, N. Pierdicca, and F. S. Marzano, "Spectral downscaling of integrated water vapor fields from satellite infrared observations," *IEEE Trans. Geosci. Remote Sens.*, vol. 50, no. 2, pp. 415–428, Feb. 2012.

[13] P. Basili, S. Bonafoni, P. Ciotti, and N. Pierdicca, "Modeling and sensing the vertical structure of the atmospheric path delay by microwave radiometry to correct SAR interferograms," *IEEE Trans. Geosci. Remote Sens.*, vol. 52, no. 2, pp. 1324–1335, Feb. 2012.

[14] A. Monti Guarnieri, S. Tebaldini, F. Rocca, and A. Broquetas, "GEMINI: Geosynchronous SAR for earth monitoring by interferometry and imaging," in *Proc. IEEE Int. Geosci. Remote Sens. Symp. (IGARSS)*, 2012, pp. 210–213.

[15] A. Ferretti, C. Prati, and F. Rocca, "Permanent scatters in SAR interferometry," *IEEE Trans. Geosci. Remote Sens.*, vol. 39, no. 1, pp. 8–20, Jan. 2001.

[16] R. F. Hanssen, "Stochastic model for radar interferometry," in *Radar Interferometry: Data Interpretation and Error Analysis*. Norwell, MA, USA: Kluwer, 2001, pp. 98–110.

[17] B. Puysségur, R. Michel, and J.-P. Avouac, "Tropospheric phase delay in interferometric synthetic aperture radar estimated from meteorological model and multispectral imagery," *J. Geophys. Res.*, vol. 112, no. B05419, pp. 1–12, May 2007.

[18] J. Dudhia, "A nonhydrostatic version of the Penn State-NCAR Mesoscale Model: Validation tests and simulation of an Atlantic cyclone and cold front," *Mon. Weather Rev.*, vol. 129, no. 5, pp. 1493–1513, May 1993.

[19] R. Ferretti, G. Mastrantonio, S. Argentini, L. Santoleri, and A. Viola, "A model-aided investigation of winter thermally driven circulation in the Italian Tyrrhenian coast for a case study," *J. Geophys. Res.*, vol. 108, no. D24, pp. 4777–4792, Dec. 2003.

[20] S.-Y. Hong and H.-L. Pan, "Nonlocal boundary layer vertical diffusion in medium-range forecast model," *Mon. Weather Rev.*, vol. 124, no. 10, pp. 2322–2339, Oct. 1996.

[21] G. L. Stephens, "The parametrization of radiation for numerical Weather prediction and climate models," *Mon. Weather Rev.*, vol. 112, no. 4, pp. 826–867, Apr. 1984.

[22] J. S. Kain and J. M. Fritsch, "Convective parameterization for mesoscale models: The Kain-Fritsch scheme," *Meteorol. Monogr.*, vol. 24, no. 46, pp. 165–170, Dec. 1993.

[23] J. S. Kain, "The Kain-Fritsch convective parameterization: An update," *J. Appl. Meteorol.*, vol. 43, no. 1, pp. 170–181, Jan. 2004.

[24] J. Reisner, R. Rasmussen, and R. Bruintjes, "Explicit forecasting of supercooled liquid water in winter storms using the MM5 mesoscale model," *Quart. J. Roy. Meteorol. Soc.*, vol. 124, no. 548, pp. 1071–1107, Apr. 1998.

[25] A. C. Lorenc *et al.*, "The met office global three-dimensional variational data assimilation scheme," *Quart. J. Roy. Meteorol. Soc.*, vol. 126, no. 570, pp. 2991–3012, Oct. 2000.

[26] P. Courtier *et al.*, "The ECMWF implementation of three-dimensional variational assimilation (3DVAR). I: Formulation," *Quart. J. Roy. Meteorol. Soc.*, vol. 124, no. 550, pp. 1783–1807, Jul. 1998.

[27] D. M. Barker, W. Huang, Y.-R. Guo, A. J. Bourgeois, and Q. N. Xiao, "A three-dimensional variational data assimilation system for MM5: Implementation and initial results," *Mon. Weather Rev.*, vol. 132, no. 4, pp. 897–914, Apr. 2004.

[28] L. Cucurull, F. Vandenberghe, D. Barker, E. Vilaclara, and A. Rius, "Three-dimensional variational data assimilation of ground-based GPS ZTD and meteorological observations during the 14 December 2001 storm event over the Western Mediterranean Sea," *Mon. Weather Rev.*, vol. 132, no. 3, pp. 749–763, Mar. 2004.

[29] C. Faccani *et al.*, "Impact of a high density GPS network on the operational forecast," *Adv. Geosci.*, vol. 2, pp. 73–79, Mar. 2005.

[30] D. F. Parrish and J. C. Derber, "The National meteorological center's spectral statistical interpolation analysis system," *Mon. Weather Rev.*, vol. 120, no. 8, pp. 1747–1763, Aug. 1992.

[31] M. K. Ramamurthy and F. H. Carr, "Four dimensional data assimilation in the monsoon region. Part I: Experiments with wind data," *Mon. Weather Rev.*, vol. 115, no. 8, pp. 1678–1706, Aug. 1987.

[32] C. Cardinali, S. Pezzulli, and E. Andersson, "Influence matrix diagnostic of a data assimilation system," *Quart. J. Roy. Meteorol. Soc.*, vol. 130, no. 603, pp. 2827–2849, Oct. 2004.

[33] F. S. Marzano, E. Picciotti, and G. Vulpiani, "Rain field and reflectivity vertical profile reconstruction from C-band radar volumetric data," *IEEE Trans. Geosci. Remote Sens.*, vol. 42, no. 5, pp. 1033–1046, May 2004.

[34] E. Picciotti, M. Montopoli, S. Di Fabio, and F. S. Marzano, "Statistical calibration of surface rain fields derived from C-band Mt. Midia operational radar in central Italy," in *Proc. ERAD*, 2010.

[35] M. K. Ramamurthy and F. H. Carr, "Four dimensional data assimilation in the monsoon region. Part II: Role of temperature and moisture data," *Mon. Weather Rev.*, vol. 116, no. 10, pp. 1896–1913, Oct. 1988.

[36] D. S. Wilks, *Statistical Methods in the Atmospheric Science*. New York, NY, USA: Academic, 1995, 467 pp.

Emanuela Pichelli received the Laurea (*cum laude*) and the Ph.D. degrees in physics from the University of L'Aquila, L'Aquila, Italy, in 2007 and 2011, respectively.

In 2011, she has a Postdoctoral Position in the group of weather modeling, Center of Excellence for Remote Sensing and Modeling of Severe Weather (CETEMPS), University of L'Aquila. Since 2013, she has been a Visiting Scientist with the Mesoscale and Microscale Meteorology Division, National Center for Atmospheric Research (NCAR), Boulder, CO, USA. She participated as Investigators to National and International Projects funded by the Italian Civil protection Department and the European Space Agency. In 2012, she has been a Coorganizer of the experimental campaign over Italy of the HyMeX project. Her research interests include mesoscale meteorology in complex terrain areas, parameterization of turbulence in numerical weather prediction models (MM5, WRF-ARW), observations integration and assimilation into weather prediction models, and mesoscale models validation through observations from different source (remote, ground-based, and *in situ* measurements).

Dr. Pichelli was the recipient of a Young Scientist Award EGU at the 10th Plinius Conference in 2008.

Rossella Ferretti received the Laurea (*summa cum laude*) in physics from the University of Rome "La Sapienza," the Ph.D. degree in geophysics from the School of Geophysical Sciences, Georgia Institute of Technology, Atlanta, GA, USA, and the Ph.D. degree in physics from Ministry of Education, Rome, Italy.

Since 1989, She has been working as a Researcher with the Department of Physics, University of L'Aquila, L'Aquila, Italy, and in 2006, she got a position as an Associate Professor with the Department of Physics, University of L'Aquila. She is an Expert in mesoscale modelling and in charge with the Real-Time forecast, University of L'Aquila. She was a Codirector with the ISSAOS Summer School on Atmospheric Data Assimilation and a Chairman of a session on Data Assimilation at EGU 2005. She was invited at the Expert Meeting of COST 720 to organize the European Campaign LAUNCH. She was responsible for several national and international projects: Regione Abruzzo for high-resolution weather forecast; Presidenza del Consiglio dei Ministri Dipartimento della Protezione Civile (DPC) for testing and tuning high-resolution weather forecast; ESA for producing high-resolution water vapor map for InSar and using via 3DVAR assimilation water vapor from InSar for improving weather forecast. She was a National Representative for COST Action: Action/TC/DC:ES0702. She acts as a Referee for several international journals: *Meteorology and Atmospheric Physics*, *Atmospheric Research*, NHESS, for the Research Council of Norway for a proposal on the Orographic precipitation, and for the Netherlands e-Science Center (NLeSC) and the Netherlands Organization for Scientific Research (NWO). She is invited to join the Editorial Board of The Scientific World Journal. She is a Guest Editor of QJRMET for the special issue of the Hymex campaign. She was acting as a Referee for FIRB Giovani national proposal. She was a nominated reviewer for the Italian Super Computing Resource Allocation promoted by CINECA. She is an Author of more than 45 papers on international journals. Since 1998, She has been teaching several courses such as dynamic meteorology and climatology.

Dr. Ferretti is a Member of the Executive Committee for Implementation and Science Coordination of the HyMex project and a coordinator responsible for the Italian Meteorological Center, L'Aquila, Italy, during the HyMex campaign.

Domenico Cimini received the Laurea (*cum laude*) and the Ph.D. degrees from the University of L'Aquila, L'Aquila, Italy, in 1998 and 2002, respectively, both in physics.

In 2002–2004, he was with the Center of Excellence for Remote Sensing and Modeling of Severe Weather (CETEMPS), University of L'Aquila. In 2004–2005, he was a Visiting Fellow with the Cooperative Institute for Research in Environmental Sciences (CIRES), University of Colorado, Boulder, CO, USA. In 2005–2006, he joined with the Institute of Methodologies for the Environmental Analysis (IMAA) of the Italian National Research Council (CNR) working on ground- and satellite-based observations of cloud properties. Since 2006, he is an Affiliate of the Center for Environmental Technology (CET), Department of Electrical and Computer Engineering, University of Colorado, Boulder, CO, USA, where in 2007 he served as an Adjunct Professor. He is currently with the Satellite Remote Sensing Division, IMAA/CNR. He participated as Investigators and Coprincipal Investigators to several international projects funded by the Italian Ministry of University and Research, the Italian Space Agency, the European Space Agency, and the U.S. Atmospheric Radiation Measurement program. Currently, he is sharing the coordination of an International Microwave Radiometer Network (MWRnet), grouping more than 20 meteorological institutions. Since 2002, he has been a Teaching Assistant for undergraduate and graduate courses in remote sensing, atmospheric sounding, technologies for aviation, and hydrogeological risks assessment.

Dr. Cimini was the recipient of the Fondazione Ugo Bordoni Award 2008 in memory of Prof. Giovanni D'Auria.

Giulia Panegrossi received the Laurea degree (*Hons.*) in physics from the University of Rome "La Sapienza," Rome, Italy, and the Ph.D. degree in atmospheric sciences from the Department of Atmospheric and Oceanic Sciences, University of Wisconsin-Madison, Madison, WI, USA, in 2004.

Since 2011, she has been a Researcher with the Institute of Atmospheric Sciences and Climate of the National Research Council of Italy (ISAC-CNR), Rome, Italy. She is an Author and Coauthor of several referred publications in International Journals and Proceedings of International Conferences. Her research interests include remote sensing of clouds and precipitation; analysis of heavy precipitation events through the use of NWP models (UW-NMS, MM5, WRF-ARW) and comparison with remote, ground-based, and *in situ* measurements; passive microwave precipitation retrieval algorithms; radiative transfer through precipitating clouds; microphysics characterization of precipitating clouds using models and observations; development of microphysics schemes; cloud electrification; and nowcasting techniques.

Daniele Perissin was born in Milan, Italy, in 1977. He received the Master's degree (laurea) in telecommunications engineering and the Ph.D. degree in information technology (cum laude) from Politecnico di Milano, Milan, Italy, in 2002 and 2006, respectively.

He joined with the Signal Processing Research Group, Politecnico di Milano, in 2002, and since then, he has been working on the Permanent Scatterers technique in the framework of Radar Remote Sensing. In 2009, he moved to the Institute of Space and Earth Information Science, Chinese University of Hong Kong as a Research Assistant Professor. Since October 2013, he holds a position as an Assistant Professor with the School of Civil Engineering, Purdue University (USA), West Lafayette, IN, USA. He is an Author of a patent on the use of urban dihedral reflectors for combining multisensor Interferometric Synthetic Aperture Radar (InSAR) data and he has published about 100 research works in journals and conference proceedings. He is the Developer of the software Sarproz for processing multitemporal InSAR data.

Dr. Perissin received the JSTARS best paper award in 2012.

Nazzareno Pierdicca (M'04–SM'13) received the Laurea (Doctor's) degree in electronic engineering (*cum laude*) from the University "La Sapienza" of Rome, Rome, Italy, in 1981.

From 1978 to 1982, he worked with the Italian Agency for Alternative Energy (ENEA). From 1982 to 1990, he was working with Telespazio, Rome, Italy, in the Remote Sensing Division. In November 1990, he joined with the Department of Information Engineering, Electronics and Telecommunications, Sapienza University of Rome. He is currently a Full Professor and teaches remote sensing, antenna, and electromagnetic fields with the Faculty of Engineering, Sapienza University of Rome. His research interests include electromagnetic scattering and emission models for sea and bare soil surfaces and their inversion, microwave radiometry of the atmosphere, and radar land applications.

Prof. Pierdicca is a past Chairman of the GRSS Central Italy Chapter.

Fabio Rocca received the Doctor Honoris Causa in geophysics from the Institut National Polytechnique de Lorraine, Nancy, France.

He is an Emeritus Professor of telecommunications with the Dipartimento di Ingegneria Elettronica, Informazione e Bioingegneria, Politecnico di Milano, Milan, Italy. His research interests include image coding, seismic signal processing for oil prospections, and synthetic aperture radar.

Dr. Rocca was the President of the European Association of Exploration Geophysicists and an Honorary Member of the Society of Exploration Geophysicists and the European Association of Geoscientists and Engineers (EAGE). He was the recipient of the Erasmus Award from EAGE, the 2012 ENI Prize for New Frontiers for Hydrocarbons, and the Chinese Government International Scientific Technological Cooperation Award for 2014.

Bjorn Rommen received the M.S. degree in electrical engineering from the Delft University of Technology, Delft, The Netherlands, in 1999.

From 1999 onwards, he has been working in the field of Earth observation with the Research and Technology Centre of the European Space Agency (ESTEC), Noordwijk, The Netherlands. Recently, he has been involved in the Sentinel-1A pre-launch and post-launch activities including the commissioning phase covering overall SAR in-orbit performance. His research interests include electromagnetics theory, computational electromagnetics, and radar remote sensing.